Open Access

Journal of Energy and Power Technology

LIDSEN Publishing Inc.

Project Report

Test Site for Small Wind Turbines – Technical and Logistical Issues of a Decade-Long Project

Rafael B. Oliva [1, 2, †, *], Andrés Zappa [3, †], Mariano Amadio [3, †], Guillermo Catuogno [4, *]

1. Universidad Nacional de la Patagonia Austral (UNPA) and L&R Ingenieria, Gregores y Lero Rivera, Rio Gallegos, Argentina; E-Mails: roliva@uarg.unpa.edu.ar; roliva@lyringenieria.com.ar
2. L&R Ingenieria, T.deLoqui 58, Río Gallegos, Argentina
3. Instituto Nacional de Tecnología Industrial, Mercado Concentrador Neuquén, Ruta Prov.7 km. 5, Neuquén, Argentina; E-Mails: azappa@inti.gob.ar; amadiom@inti.gob.ar
4. Laboratorio de Tecnologias Apropiadas (LabTA), Universidad Nacional de San Luis, Villa Mercedes (San Luis), Argentina; E-Mail: grcatu@ieee.org

† These authors contributed equally to this work.

* **Correspondences:** Rafael B. Oliva and Guillermo Catuogno; E-Mails: roliva@uarg.unpa.edu.ar; roliva@lyringenieria.com.ar; grcatu@ieee.org

Academic Editors: Cher Ming Tan and Grigorios L. Kyriakopoulos

Journal of Energy and Power Technology
2025, volume 7, issue 2
doi:10.21926/jept.2502009

Received: October 31, 2024
Accepted: April 09, 2025
Published: May 05, 2025

Abstract

This work addresses the main results of a test site for small wind turbines (SWTs) located in Patagonia, and the development of the measurement systems involved, including the uncertainties calculations according to applicable IEC standards. Due to market evolution for over a decade, the test systems evolved from battery-charging SWTs to grid-connected units. The test site, developed and managed by state-owned INTI (National Institute for Industrial Technology), was established in 2012 and received support from the local Curtail-Co municipality and other institutions. Since its creation, it has thrived in aiding local manufacturers of SWTs in certifying their machines, providing power-curve measurement facilities, duration testing, and sound emissions testing. It has also provided design

recommendations and improvements related to optimizing energy capture and reliability of SWTs.

Keywords
Wind energy; power conversion; small wind turbines; measurements; test site

1. Introduction

Small wind turbines (SWTs) play an important role in renewable energy production, especially in regions where the wind resource is significant, and their power production can compete with or supplement solar photovoltaic solutions. These machines, according to the IEC 61400 Standard series [1] definitions, comprise wind turbines for electric power production with a swept area of up to 200 m^2, and operate as stand-alone battery charging or grid-connected [2]. A discussion of the IEC 61400 series and its definition of wind classes for the design and testing of wind turbines can be found in [3].

Worldwide, several facilities have been established as test sites explicitly dedicated to SWTs, with the mission of evaluating and improving the performance, safety, and reliability of these systems. The National Renewable Energy Laboratory (NREL) in the US pioneered many of these efforts to conduct comprehensive testing of SWTs, covering aspects such as duration, power performance, safety, and noise emissions [4, 5]. In the same region, the Small Wind Certification Council (ICC-SWCC™) [6], an independent ISO/IEC 17065 accredited certification body, certifies SWTs to meet or exceed the requirements of specified standards, primarily based on older AWEA (American Wind Energy Association) and more recent IEC standards. In Australia, other test sites were established such as the ResLab Field Test Site [7] and the National Small Wind Turbine Centre (NSWTC) [8]. In Europe, Spain has participated through CIEMAT in early efforts [9] to establish world-class test sites for SWTs such as CEDER in Lubia, Spain. Others, such as Intertek, have established test sites both in Spain [10] and Sweden [11]. These test sites employ rigorous procedures based on international standards to assess various turbine characteristics. The data collected from these tests are valuable both for manufacturers (to optimize their products) and for end users.

The INTI SWT-Testing Laboratory, established in 2012 [12], is one of the few facilities installed in South America and is located near the city of Cutral-Có, Neuquén province in Argentina. Using two meteorological towers, the installed measurement system is designed to obtain the power curve of four wind turbines simultaneously. The systems under test were initially off-grid type SWTs for battery charging, later evolving to grid-connected turbines. The facilities were built by initiative of the INTI Neuquén center as part of a strategy to promote SWTs produced in Argentina, bringing together wind turbine manufacturers (more than fifteen in 2011) to agree on common evaluation and measurement methodologies by international standards such as IEC 61400-12-1 [1] and equipment labeling initiatives such as IEA Task 27 “Consumer Labeling of Small Wind Turbines” [13]. In this initiative, two former group leaders at INTI, Guillermo Martin and Juan Pablo Duzdevich, had a decisive role from the first studies in 2010, and much of their pioneering work allowed the SWT-Testing Lab to develop and interact with similar institutions worldwide. The performance tests were part of an INTI program covering aspects such as design, marketing, and production of turbines,

seeking to build a technical reference in SWTs, providing users with reliability information, and promoting the use of this type of generation systems.

The laboratory's initial objective (Figure 1) was to standardize the testing of locally manufactured SWTs to provide potential users with reliable elements for comparing different types of equipment. In addition, several aspects of the equipment's operation and safety were later analyzed, which allowed manufacturers to improve their designs.

Figure 1 The INTI SWT Testing Laboratory location in Argentine Patagonia, elevation and wind data.

The laboratory facilities comprise a 5,000 m^2 site with a perimeter fence and a 120 m^2 building that houses the necessary equipment, workshop areas, and offices. Up to four wind turbines can be simultaneously evaluated, mounted on independent retractable towers at 9 m height. It also has two meteorological towers with conventional wind measurements at 9 and 18 m height. The maximum admissible power currently is 10 kW and was initially configured for testing wind systems in battery charging configuration [12], later expanding to grid-connected SWTs after the legislation supporting this possibility [14] was enforced.

The measurement system consists of a meteorological variables measurement module, an electrical variables measurement module, and a data acquisition system that synchronizes, pre-processes, and stores the data obtained from the various sensors. The meteorological module consists of a grid tower with an anemometer, a wind vane, a thermometer, and a barometer, all mounted following the requirements of Annex G of the IEC 61400-12-1 standard [1]. The original SWTs were tested in battery charging configuration, in which the electrical module requires a bank of dump resistors, a regulator to configure the test voltage, and a battery bank to maintain this voltage at the level defined for each stage of the test ([1], Annex H). The data acquisition system can synchronize measured data, both electrical and meteorological. It also carries out preliminary statistical processes to create databases used to obtain the results provided in the standard. The placement of each wind turbine and each instrument on the site (Figure 2) and the subsequent processing of the data requires compliance with certain criteria set out in the standard, which cover topographical aspects, sizing, and position of the equipment and obstacles.

Laboratory description and distribution

Lab Specifications	
SWTs under test	*4*
SWT Configuration	Stand Alone Battery charging and grid-connected
Power Range	500 W – 10 kW
Met towers	9 m – 18 m
Reference Logger	Nomad2 SecondWind / Vaisala

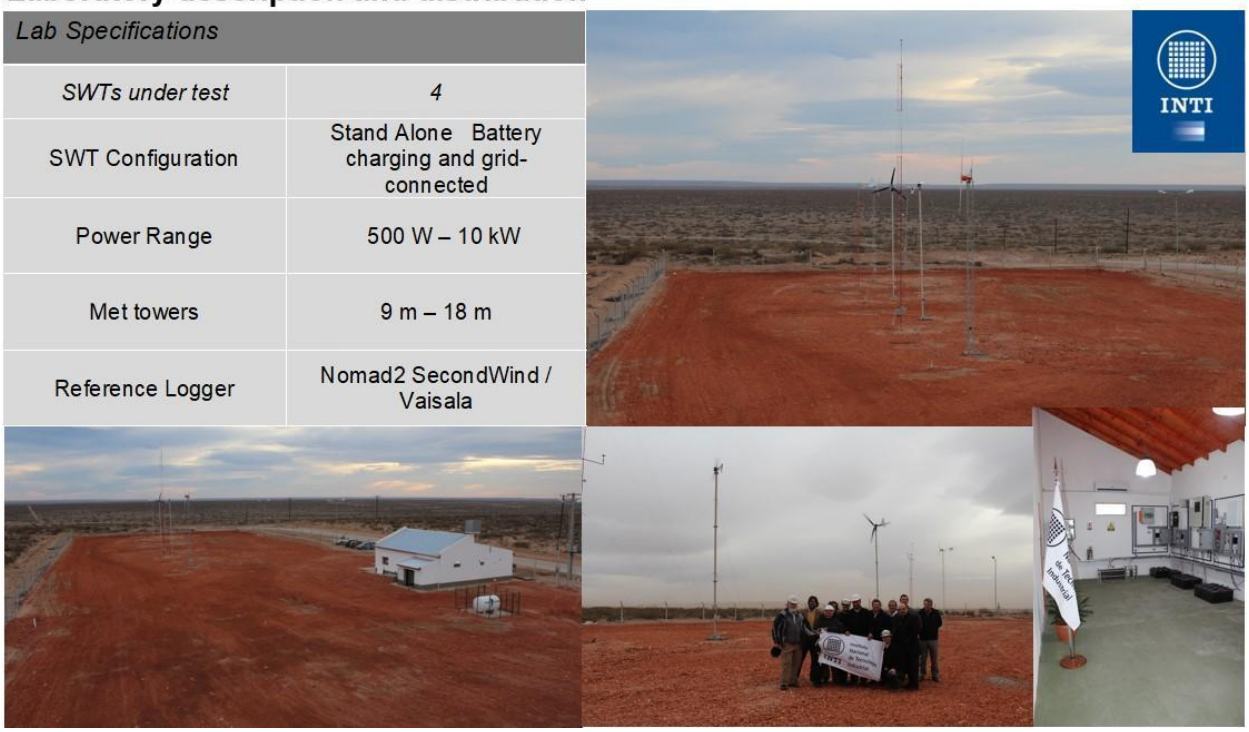

Figure 2 The INTI SWT Testing Laboratory description and distribution.

2. Materials and Methods

2.1 Power Curve Measurement

2.1.1 Principles Behind the Measurement of Power in Wind Turbines

The well-known basic relationship between the actual power output of a wind machine and the wind speed [15, 16] can be expressed as:

$$P = \frac{1}{2}\rho S \eta C_p V^3 \quad [W] \tag{1}$$

Where ρ is the air density (nominally 1.225 kg/m^3), S is the surface swept by the wind turbine rotor, η is the generator and mechanical transmission efficiency (assumed constant), C_p is the dimensionless aerodynamic coefficient of rotor power (dependent on the wind and rotation speed), V is the wind intensity in meters per second, and P is the power in W. In addition to the cubic relationship with the wind intensity, and assuming S and η constant, the shape of the $P(V)$ curve depends mainly on the C_p coefficient (with its maximum value limited to 0.593, known as Betz limit [15]), and to a lesser extent on the variations in air density with temperature and atmospheric pressure. This last relationship can be written as follows:

$$\rho = \frac{100 * B}{RT} \quad \left[\frac{kg}{m^3}\right] \tag{2}$$

Where B is the atmospheric pressure in hPa, T is the temperature in K, and R is the gas constant of dry air equivalent to 287.05 J/kg·K. The adjustment coefficient of 100 is unit related.

As seen from (1) and (2), the measurement of the *P(V)* curve must consider the wind speed acquired with an anemometer at hub height, the electrical power produced, the temperature, and barometric pressure. Due to the interference of the meteorological measuring tower, a direction sensor (vane) is also included. In addition, in the case of large wind turbines, more than one anemometer is added at different heights.

The procedures for determining the power curve for grid-connected machines are specified in [1] (and later editions), using the statistical *method of bins* (see section 3.2) and assume that the grid absorbs all the electric power that the wind turbine can produce, resembling the normal operating condition of this equipment. This assumption considerably simplifies the methodology for determining the power curve.

In the case of SWTs connected to a battery bank, the electrical layout will determine the testing method. Most SWTs use a permanent magnet synchronous generator connected to a three-phase rectifier (a detailed model of this configuration is explained in [15], chapters 7 and 8). The voltage of the batteries influences the rotational speed of the rotor, consequently, the power coefficient C_p has a dependency on this parameter. The effective resistance presented by the battery and load combination varies in a non-linear manner. This implies that the amount of power that can be absorbed from the wind will depend on the battery's charge level and the voltage regulator's configuration, which complicates the procedure required to determine the power curve [17]. A compromise was reached in IEC 61400-12-1, Annex H [1] by specifying mandatory SWT tests at a nominal battery voltage and two optional tests at a specified "low voltage" and "high voltage." The firmware of the INTI test system accommodates options for collecting data for the mandatory and the two optional tests.

Notably, the world market for low-power wind systems is several orders of magnitude smaller than that of grid-connected machines, and its development has been comparatively slow. Thus, the standards for small wind machines advanced much slower. In the case of [1], the testing of low-power machines was included as Annex H in 2005.

2.1.2 Laboratory Set Up at the Cutral Có INTI Test Site

A detailed layout of each station can be seen in Figure 3, and the design of the meteorological data subsystem can be seen in Figure 4. The system has as its fundamental components the METEO units that measure wind, temperature, and atmospheric pressure, the PWRC/2 units that take this data and integrate it with the power measurements of the corresponding wind turbine, the battery bank, the HMI/PC unit that gathers the data and configures the load regulation, and the charge regulators with their dissipation resistors. An Ethernet network links the equipment to the individual status of each test via the Internet. A reference station is also included for measuring wind data with anemometers with Measnet calibration [3, 18, 19] at 2 heights, communicated with the HMI/PC unit, whose distribution is shown in Figure 4. Both the reference station and the PWRC/2 units communicate with the central HMI/PC system through the Modbus [20] protocol, in the first case through an RS485 link and in the second through RS232 to Ethernet converters.

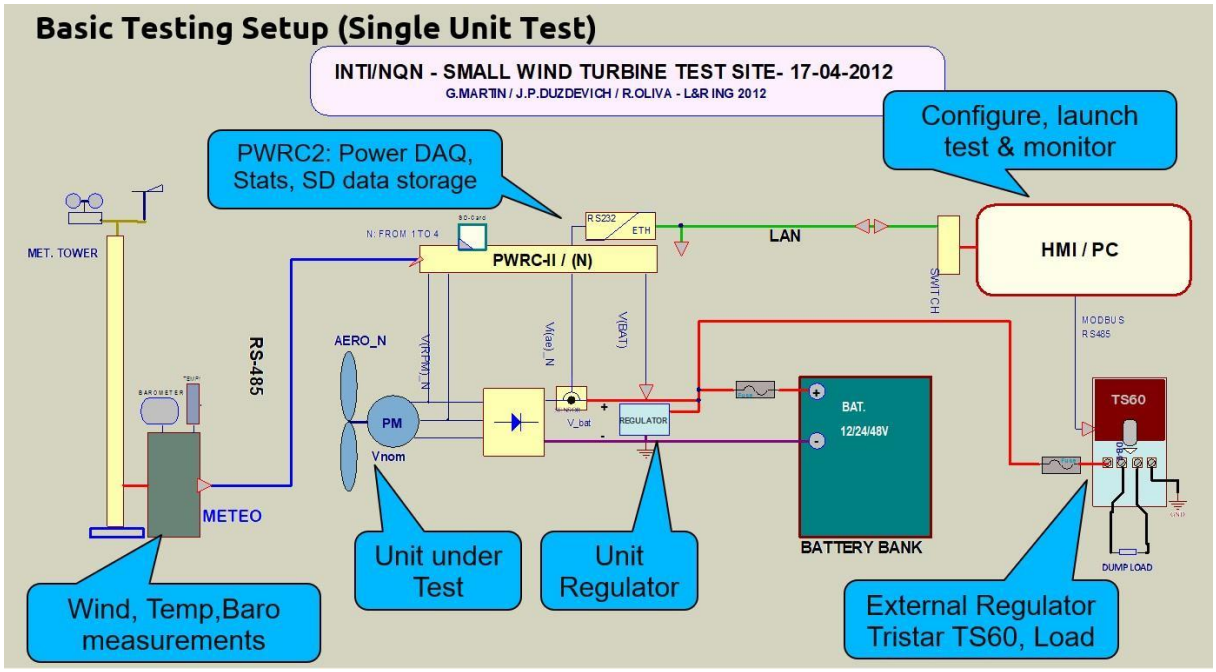

Figure 3 Basic single unit PWRC/2 + METEO testing setup.

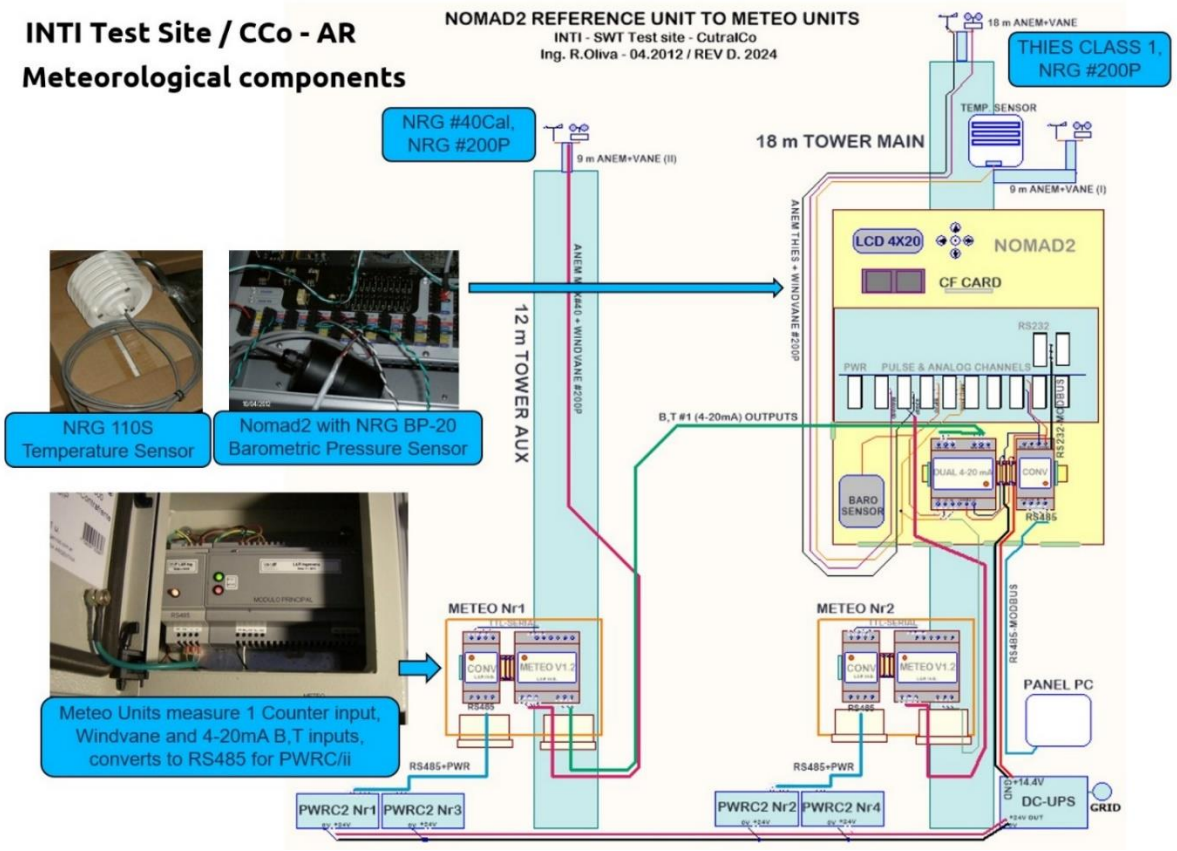

Figure 4 Distribution of the meteorological data subsystem with METEO units and Vaisala/Secondind Nomad2 unit.

2.2 Measurement System

2.2.1 Main Components of the Measurement System

Both the PWRC/2 and METEO equipment are an evolution of the first PWRC [17] units developed in 2005 by L&R Ingeniería for the PERMER pilot project in Chubut, under guidelines established by the CREE (Regional Wind Energy Center, Rawson - Chubut) [21] as a program that involved installing equipment to verify the power curve in low-power wind turbines in remote areas of the province of Chubut [22]. The imported CPU units were replaced by locally manufactured CL2bm1 boards [23] that have proved to be highly reliable and have storage on 2 GB SD flash memory cards (Figure 5). These boards [24] have been in use since 2012, operating continuously except for firmware updates.

The technical characteristics of the measurement system are summarized below:

- Wind turbines under test: 4 (four).
- Test power range: 500 W to 10 kW.
- Operating wind speed range: 1 to 75 m/s.
- Operating Temperature Range: -55°C to 60°C.
- Measurement of direct current electrical output power.

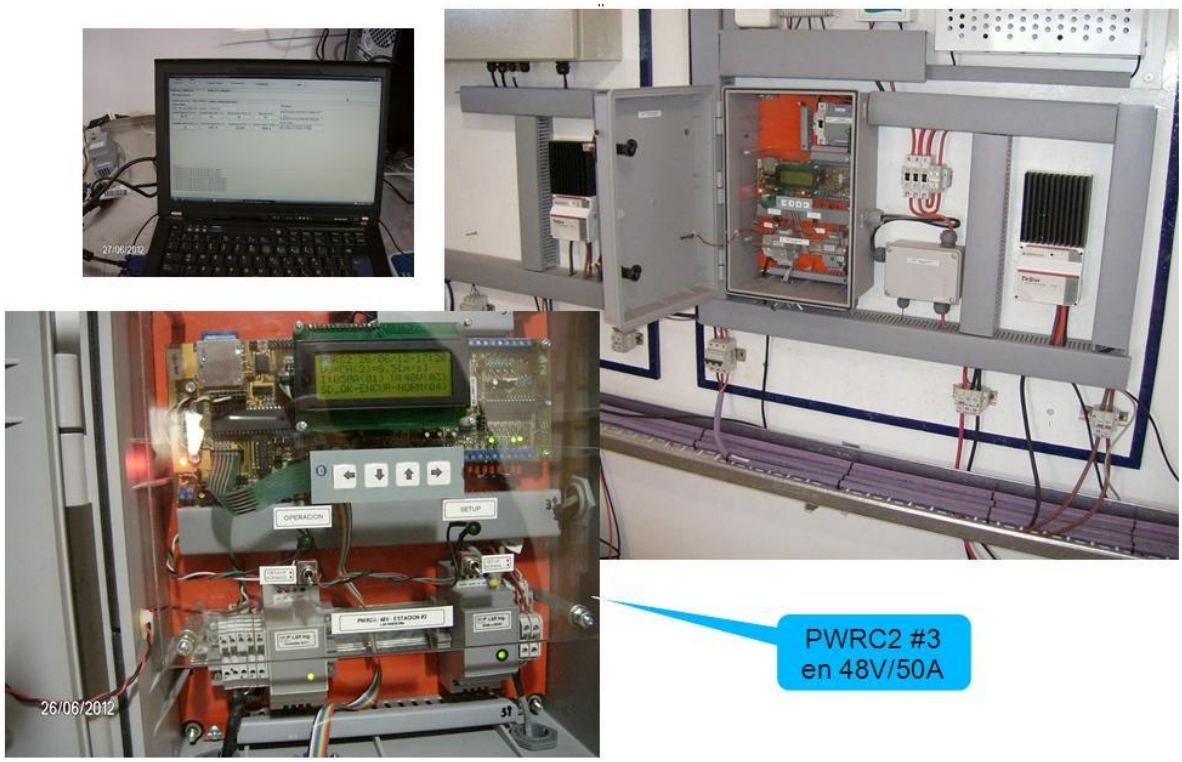

Figure 5 A view of the original layout of one of the four PWRC/2 stations and the HMI/PC interface.

2.2.2 Uncertainties Analysis in the Measurement System

Since the publication in 1993 of the ISO - Guide to the Expression of Uncertainty in Measurement or GUM [25], the concept of uncertainty and the way of quantifying it were established to give meaning to the expressions of a measurement. The various components of uncertainty were classified into two large groups (A and B) according to the methodology with which they were

evaluated (regardless of their origin) as random or systematic errors, and the concepts of *combined standard uncertainty* and *expanded uncertainty* were conceived [26] to study the propagation of uncertainties (formerly error propagation), in addition to a methodology for reporting uncertainty in a measurement. In the case of this work, the IEC 61400-12-1 standard [1] in Annexes D, and E provides a detailed description of the methodology for evaluating uncertainties for the measurement of the power curve of high and low power wind generators. Its application to low-power measurement systems has been described in [27] and in [28].

Regarding the sources of uncertainty of the measurement system:

1. Uncertainties in the measurement of wind speed and direction. Associated with the calibration and assembly of instruments and distortion of wind flow through the terrain.
2. Uncertainties in DC current and voltage measurement. Associated with the calibration and type of transducers used, and with the *P=V*I* product performed in single precision floating point.
3. Uncertainties in atmospheric pressure and temperature measurement. Associated with the type and assembly of instruments.

More detailed information about the procedure to evaluate uncertainties in the PWRC/2 system and the report procedures will be discussed in section 3.3.

3. Test Execution and Reporting

3.1 Execution of Tests, Power Curve Reports

Power curve testing allows the evaluation of the power generation of a wind turbine based on the wind speed, as well as estimating the annual energy production in different wind conditions. This process includes simultaneous measurements of meteorological data and power production. To do so, several aspects must be considered.

First, the choice of test site must be evaluated carefully. The location of the wind turbine for testing must be representative of the wind resource to be analyzed. Ideally, the terrain should be flat and free of obstructions, as any topographical irregularities can distort measurements. In cases where there are slopes or irregular terrain, a pre-calibration of the site is performed to adjust the wind readings, ensuring that they correctly reflect the conditions on the rotor.

To obtain accurate wind speed readings, the wind turbine must be prevented from blocking the airflow to the anemometer. This involves defining exclusion sectors where the wind, by hitting the rotor before reaching the anemometer, could reduce the measured speed compared to the actual speed. These sectors are defined for each installation, ensuring that the recorded wind represents what is impacting the wind turbine (Figure 6).

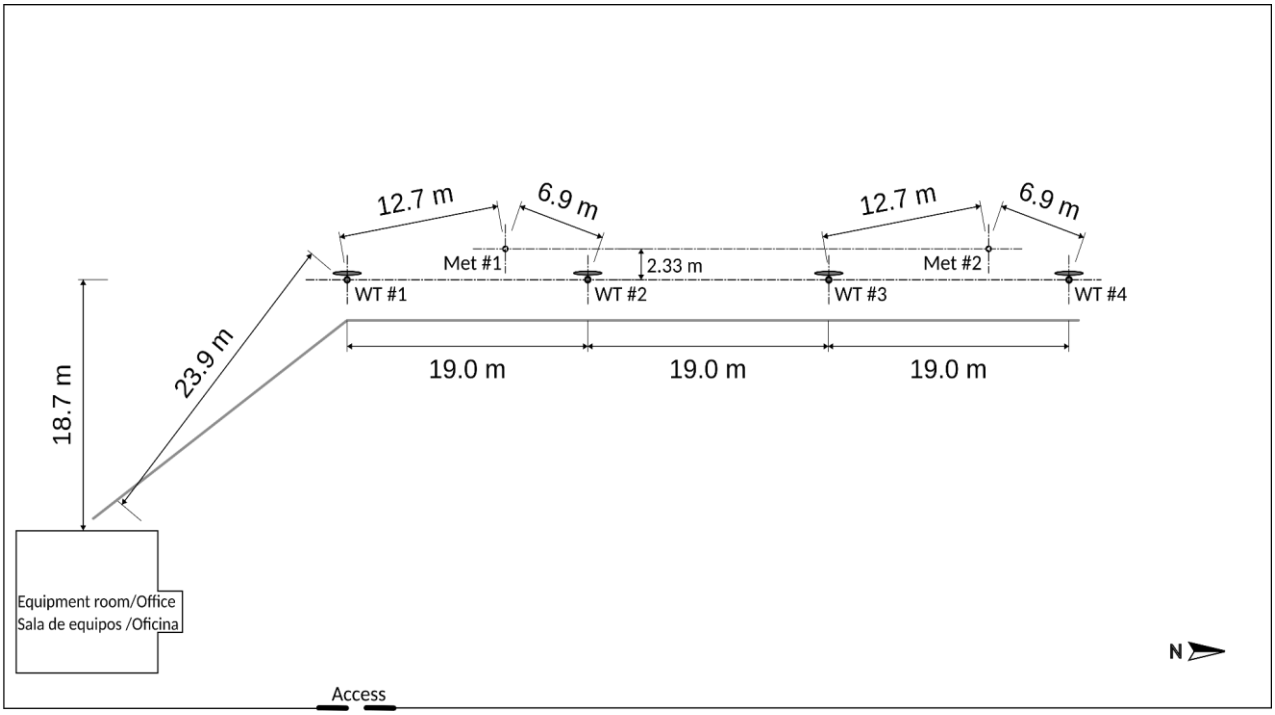

Figure 6 Plan view of the distribution of meteorological measuring towers and wind turbines. Cutral-Có (Neuquén).

At the measurement system configuration stage, the valid measurement ranges for each parameter (wind speed, direction, pressure, temperature, voltage, and current) are determined. The configuration of the measurement systems must ensure consistency between the wind readings and the generated electrical data, minimizing interference and measurement errors.

3.2 Measurement Configurations

Once the system is configured, simultaneous measurements of wind speed, direction, pressure, temperature, and electrical variables (voltage and current) generated by the wind turbine are carried out at a frequency of 1 Hz. This means that several variables are recorded per second, ensuring an accurate and detailed reading of changes in the wind resource and the response of the equipment.

Given the large volume of data captured, an averaging process is performed in the firmware that groups the information into one-minute intervals. Each minute of valid data is recorded as an average, along with the maximum, minimum, and standard deviation of the power generated. This simplifies the interpretation of the data and allows a graphical representation of the different operating modes of the wind turbine over time. For high-power wind turbines in [1], the averaging interval is 10 minutes, but for SWTs, the required interval in Annex H is 1 minute.

The data obtained from the electrical and meteorological modules are processed to determine their eligibility. Only data in which the wind incident on the wind turbine or meteorological tower is not obstructed by any surrounding objects are used to build the power curve. To ensure this, directions in which the airflow is disturbed are excluded for each test position. This procedure is carried out following the guidelines defined in Annex A of the IEC 61400-12-1 [1] standard.

The data are sampled at a frequency of 1 Hz, and before being stored, the maximum, minimum, average, and standard deviation values are obtained in the pre-processing stage. These minute data are presented as "scatter plots" in the results section. Additionally, corrections are required in the air density values obtained from the pressure and temperature readings for normalization to a reference density. Finally, in the case of low-power turbines with furling control, a speed normalization is performed according to the following expression:

$$V_{norm} = V_{1min}\left(\frac{\rho_{1min}}{\rho_0}\right)^{\frac{1}{3}} \quad \left[\frac{m}{s}\right] \tag{3}$$

Where
V_{norm} is the normalized speed,
V_{1min} is the average speed over the measurement period of one minute,
ρ_{1min} is the calculated density of air at the measured *B, T,*
ρ_0 is the reference density at sea level, 1.225 kg/m^3.

The IEC61400-12-1 [1] requires the use of the *bins method* and keeping a record of the completeness of the test that differs between large machines and those included in Annex H (SWTs). Once the wind speed and power averages have been calculated, the method stipulates that the normalized wind and power results (V_s, P_i pairs) are to be grouped by software for each bin *i*, according to their V_s value, obtaining within each bin (whose usual width is 1 m/s) a n_i number of V_{ij}, P_{ij} pairs. The result of averaging the values within each bin "*i*" produces a pair, through the formulas:

$$V_{pi} = \frac{1}{n_i}\sum_{j=1}^{n_i} V_{ij}\,; \quad P_{pi} = \frac{1}{n_i}\sum_{j=1}^{n_i} P_{ij} \tag{4}$$

This provides the pair *"i"*, of the $P(V_i)$ table, which can be built in tabular or graphic form, and also normalized to find the power coefficient $C_p(V)$ curve, graph the pairs with their variation range or obtain a scatter-plot of measured points, which must be included as part of the test report.

3.3 Uncertainties in Power Curve Measurements

The analysis of measurement uncertainties [29] is similar to the one used in [1] Annex E for full-size grid-connected turbines, except for power measurement in PWRC/2 units, where modifications were made regarding the separate measurements of current and voltage in specific circuits, and empirical equations were derived considering the product of both magnitudes to calculate the power.

The use of the *bins method* also influences the treatment of uncertainties. To model the power curve, the (unknown) measurement function *f* is constructed, which has the basic dependencies expressed as:

$$f = f(U, I, V, B, T, SAD) \tag{5}$$

Where SAD has been added as a generic variable related to the measurement system, in [29] an expression of the combined standard uncertainty of the *P(V)* curve called $u_{c,i}^2$ for each pair *"i"*, of the table $P(V_i)$ is derived. This reflects the fact that depending on the "zone" of the curve in which

the machine is working, the uncertainties are different. The standard also considers that the components of category A are mutually independent, and the components of category A and B are mutually independent (quadratic sum). At the same time, there will be components of category B that are in full mutual correlation (e.g. resistors in series in a voltage divider). With these simplifications, determining the standard uncertainty of the elements of a $P(V_i)$ table will be given by:

$$u_{c,i}^2 = s_{P,i}^2 + u_{P,i}^2 + c_{V,i}^2 u_{V,i}^2 + c_{T,i}^2 u_{T,i}^2 + c_{B,i}^2 u_{B,i}^2 \tag{6}$$

Barometric Pressure Uncertainty Type B is considered $u_{B,i}$, and temperature $u_{T,i}$. The sensitivity coefficients for the power-related elements are unitary $c_{P,i} = 1$, and an estimate of the others ($c_{V,i}$, $c_{B,i}$, $c_{T,i}$) can be found in [29], and listed in Table 1. The uncertainties related to the data acquisition system are evaluated within the uncertainty of each parameter. For the case of electrical power, the uncertainties $u_{P,i}$ are derived from the standard, and use the relationship

$$P = VI \quad [W] \tag{7}$$

And the associated uncertainty then arises from the expression:

$$U^2(P) = \left(\frac{\partial P}{\partial V}\right)^2 (\Delta V)^2 + \left(\frac{\partial P}{\partial I}\right)^2 (\Delta I)^2 \quad [W^2] \tag{8}$$

The elements of Eqn. (8) are implementation dependent. For the measurement of current I in PWRC/2s, for example, a measurement equation similar to (5) is constructed and works as a simplified mathematical model of the input circuit system [29].

$$I = \frac{1}{S}\left[\frac{V_{REF} D}{G(2^N - 1)} - V_{o(q)}\right] = f(S, V_{REF}, D, G, V_{o(q)}) \tag{9}$$

Where
I is the current to be measured in [A],
S is the sensor sensitivity in [mV/A],
V_{REF} is the ADC reference voltage,
N is the number of bits in the ADC,
G is the circuit gain,
D is the value of the digital word (0 to 8191 in decimal) produced by the ADC,
$V_{0(q)}$ is the value of the signal offset with 0 A circulating are listed in Table 1.

Table 1 IEC A- and B-type uncertainty components list for measurement, in PWRC/2.

Category B: Instruments	**Uncertain**	**Sensibility factor**	**Uncertainty equation**
Power generated	u_{Pi}		
Current transformers	$u_{P1,i}$		
Voltage transformers	$u_{P2,i}$		
Power transducer (*)	$u_{P3,i}$	$c_{P,i} = 1$	$u_{P1,i}$ = -6E-12P_i^4 + 3E-08P_i^3 - 6E-05P_i^2 + 0.081P_i + 2.664
Power measurement system	$u_{P4,i}$		$u_{Pd,i}$ = 0.001*2185 (0.1% measuring range)
Wind speed	$u_{V,i}$		
Anemometer	$u_{V1,i}$	$c_{V,i} = \frac{\lvert P_i - P_{i-1}\rvert}{\lvert V_i - V_{i-1}\rvert}$	$u_{V1,i}$ = 0.1
Operational characteristics	$u_{V2,i}$		$u_{V2,i}$ = (0.05 + 0.005*V_i)*k/√3; where k = 2.4
Mounting effects	$u_{V3,i}$		$u_{V3,i}$ = 0.01*V_i
Air density			
Temperature	$u_{T,i}$	$c_{T,i}$ = P_i/288.15 K	
Temperature sensor	$u_{T1,i}$		$u_{T1,i}$ = 1.425/√3
Radiation protection	$u_{T2,i}$		$u_{T2,i}$ = 2
Mounting effects	$u_{T3,i}$		$u_{T3,i}$ = 1
Air pressure	$u_{B,i}$	$c_{B,i}$ =P_i/1013 hPa	
Pressure sensor	$u_{B1,i}$		$u_{B1,i}$ = 15/√3
Mounting effects	$u_{B2,i}$		$u_{B2,i}$ = 1
Data acquisition system	$u_{d,i}$		$uV_{d,i}$ = 0.001*70
Signal transmission	$u_{d1,i}$	The sensitivity factor is determined from the uncertainty of the parameter.	
System accuracy	$u_{d2,i}$		
Signal conditioning	$u_{d3,i}$		
Category B: Terrain			
Flow distortion due to terrain	$u_{V4,i}$	$c_{V,i}$	$u_{V4,i}$ = 0.03*V_i
Category B: Method			
Method	$u_{m,i}$		
Air density correction	$u_{m1,i}$	$c_{T,i}$ y $c_{B,i}$	
Category A: Statistics			
Electrical power	$s_{P,i}$	$c_{P,i}$ = 1	
Climate variations	s_W		

A similar expression is derived in [29] for the input voltage sensor chain. The complete set of equations, including the other sources of uncertainty such as wind, and air density (via temperature and barometric pressure), following the IEC 61400-12-1 methodology, is described in [27] and has been in use for the computations and data post-processing at the INTI Test Site. The list of uncertainty components is shown in Table 1. The traditional methodology supposes grid-connected machines with current and voltage transformers, not used in PWRC/2. The derived equation for the power transducer is indicated with a (*) symbol in this table.

3.4 Power Curve Calculation

The first visual result obtained is a scatter plot. Figure 7 represents the power generated as a function of the average wind speed for each recorded minute (average, maximum, minimum, and standard deviation), showing the behavior of two wind turbines under various conditions. Through the scatter plot, it is possible to identify key moments, such as the start of generation, maximum power, and the activation of the power/speed regulation system (usually a furling mechanism in SWTs).

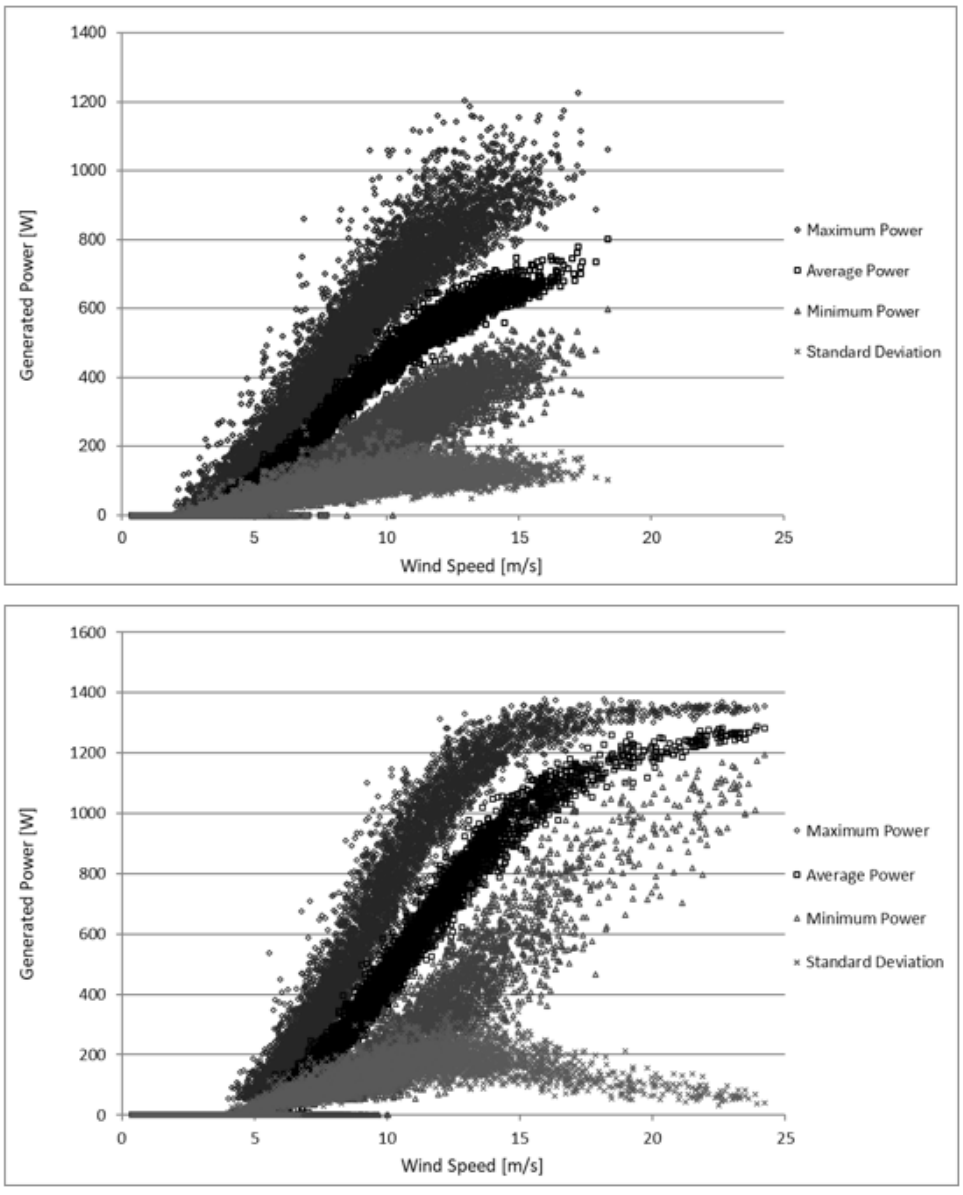

Figure 7 Scatter plot of power readings of two different wind turbines tested at the INTI-Cutral Có Laboratory (Top: Commercial Piggot type 2.4 m diam., 700 W nom. SWT, Bottom: PM 2.15 m diam., 1.2 kW nom.).

Not all measurements obtained are valid for calculating the power curve. Readings affected by obstacles in different directions, errors in the measurement system or external situations, such as wind turbine shutdowns outside the control of the test, are eliminated from the analysis. This

filtering ensures that only data representative of the actual operation of the equipment are considered (Figure 8).

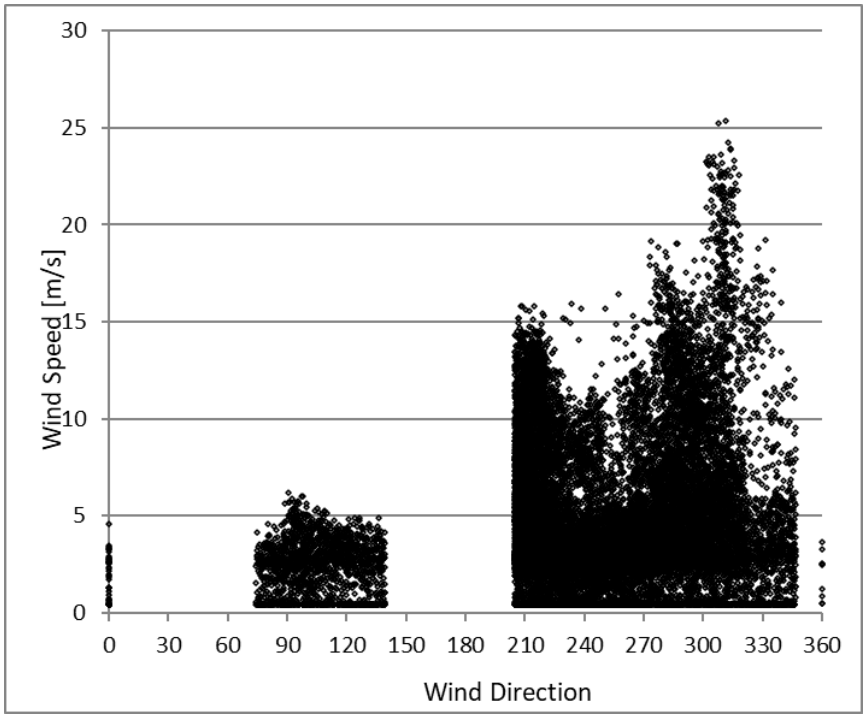

Figure 8 Filtering of valid wind measurements as a function of wind direction (Commercial Piggot type 2.4 m diam., 700 W nom. SWT).

3.5 Power Curve, Uncertainties, and Results Analysis

The final power curve is calculated from the average of the filtered scatter plot values. This average gives a clear and accurate view of the wind turbine's performance concerning wind speed and is used as a reference to compare equipment and analyze its effectiveness. Since air density (and therefore wind kinetic energy) varies with pressure and temperature, it is necessary to normalize the curve to make the results independent of these conditions. This normalization allows comparing curves obtained at different locations and times, providing an everyday basis for evaluating the performance of the wind turbine under various conditions. The calculated uncertainties for each bin are graphed at each point as vertical bars.

By comparing the generated electrical power with the kinetic power of the wind, the power coefficient C_p is calculated. This coefficient indicates the aerodynamic efficiency of the wind turbine. It shows how close the performance of the SWT is to the theoretical maximum use of wind power or Betz limit (C_{pmax} = 0.593), as mentioned in 2.1. A high C_p value, close to 0.45 is typical of larger wind turbines. It indicates an efficient design of the wind turbine and a good performance of the complete system, considering the rotor and other subsystems. SWTs rarely exceed a value of 0.3, as shown in Figure 9 for two different tests.

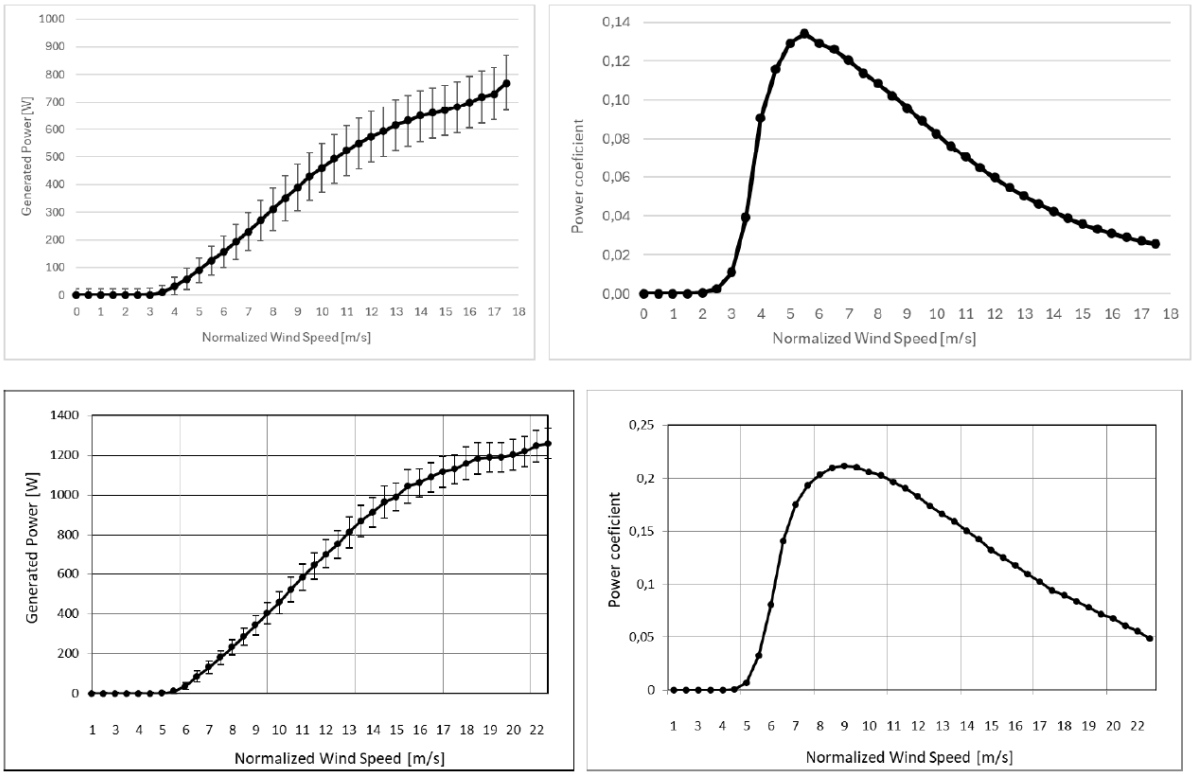

Figure 9 Power Curves with calculated uncertainties and corresponding Cp curves for two different SWTs tested at INTI Cutral Có, following [13] Annex H (Top: Commercial Piggot type 2.4 m diam., 700 W nom. SWT, Bottom: PM 2.15 m diam., 1.2 kW nom.).

By analyzing the data and scatter plots, it is possible to observe how each equipment responds at different wind speeds. Operating modes, such as generation start and protection limitations, are crucial to understanding the advantages and disadvantages of each wind turbine model.

3.6 Example Test Implementation, Power Curve and Predicted AEP (Annual Energy Production)

As an example of the typical testing sequence, the conditions for an INVAP IVS 4500 48 V machine for battery charging, and some of the results are shown in Figure 10 and Figure 11.

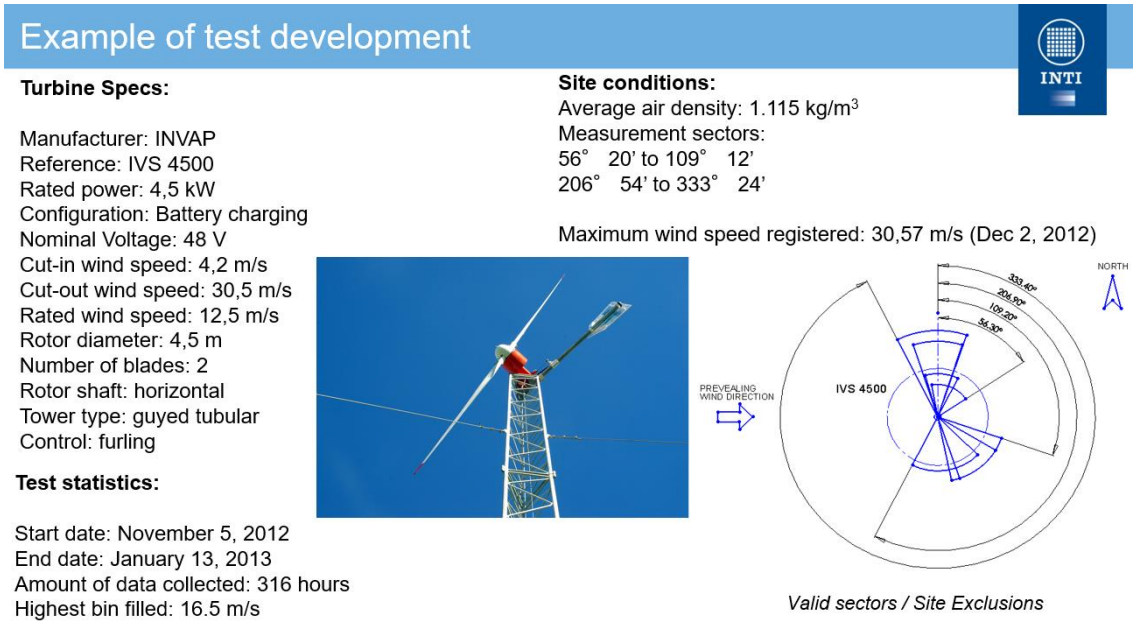

Figure 10 Testing of an INVAP IVS4500 4.5 kW SWT - information, showing partial test results at INTI Cutral Có.

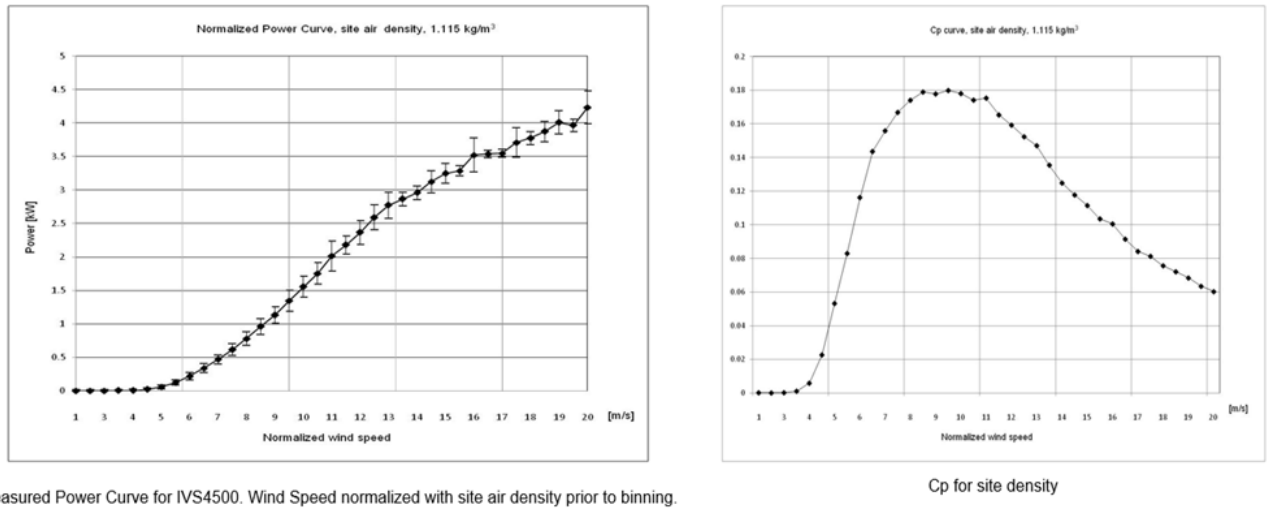

Measured Power Curve for IVS4500. Wind Speed normalized with site air density prior to binning.

Cp for site density

Figure 11 Testing of an INVAP IVS4500 4.5 kW SWT - power and Cp curve, at INTI Cutral Có.

Using the normalized power curve, the annual energy production (*AEP*) that the SWT would generate under certain wind conditions can be estimated, using the methodology indicated in [1] Annex H. To do this, the curve is applied to a standardized wind distribution, usually the Rayleigh distribution. This calculation is performed for different average wind speeds, enabling the prediction of annual energy production of turbines based on their real-world performance in various wind conditions. The results of the partial test are shown in Figure 12, rows shown in shade indicate the incomplete bin sections.

MEASURED POWER CURVE

Reference air density: 1.115 kg/m³

BIN N°	Hub height wind speed [m/s]	Power output [W]	Cp	N° of data sets (1 min. avg.)	Category A Standard uncertainty s_i [W]	Category B Standard uncertainty u_i [W]	Combined uncertainty Standard uncertainty u_c [W]
0	1.01	0.00	0.00	5964	0.09	19.62	19.62
1	2.51	0.02	0.00	2186	0.27	19.62	19.63
2	3.00	0.07	0.00	2294	0.42	19.62	19.63
3	3.49	0.46	0.00	2105	1.08	19.62	19.65
4	3.98	3.31	0.01	1227	2.72	19.66	19.85
5	4.46	17.95	0.02	809	5.53	20.63	21.36
6	4.96	57.55	0.05	486	8.41	26.89	27.98
7	5.47	120.65	0.08	334	10.91	35.08	36.74
8	5.94	216.46	0.12	259	13.04	54.55	56.09
9	6.43	338.51	0.14	232	14.77	69.05	70.61
10	6.96	466.36	0.16	234	16.12	69.87	71.70
11	7.46	614.28	0.17	224	17.26	89.14	90.80
12	7.96	778.67	0.17	221	18.43	102.96	104.60
13	8.45	957.55	0.18	240	20.33	119.27	120.99
14	8.95	1131.26	0.18	257	21.60	118.51	120.46
15	9.44	1344.39	0.18	262	23.14	153.19	154.93
16	9.94	1551.70	0.18	275	24.37	154.78	156.69
17	10.43	1752.74	0.17	241	25.45	158.74	160.77
18	10.90	2013.52	0.18	251	25.74	221.15	222.65
19	11.41	2178.09	0.17	172	26.97	136.01	138.66
20	11.87	2365.31	0.16	183	27.23	174.46	176.57
21	12.42	2588.25	0.15	148	26.87	184.16	186.11
22	12.85	2771.32	0.15	88	27.51	194.03	195.97
23	13.36	2867.09	0.14	71	27.10	97.74	101.43
24	13.87	2958.23	0.12	55	26.68	96.11	99.75
25	14.41	3125.76	0.12	47	26.87	162.99	165.19
26	14.86	3245.88	0.11	32	26.44	144.83	147.23
27	15.29	3286.58	0.10	14	26.94	67.92	73.06
28	15.81	3523.52	0.10	13	24.72	256.07	257.26
29	16.33	3536.75	0.09	13	27.24	51.20	57.99
30	16.81	3548.04	0.08	7	25.35	51.20	57.13
31	17.26	3708.97	0.08	3	23.47	217.10	218.37
32	17.78	3774.17	0.08	4	23.70	92.29	95.28
33	18.22	3872.18	0.07	5	25.95	147.69	149.95
34	18.76	4009.55	0.07	2	21.31	170.50	171.82
35	19.17	3964.90	0.06	1	22.46	90.00	92.76
36	19.93	4233.62	0.06	1	17.71	245.45	246.08

Estimated annual energy production
(database A)
Reference air density: 1,115 kg/m³
Cut-out wind speed 25 m/s

(extrapolation by constant power from last bin)

Hub height annual average wind speed (Rayleigh)	AEP-measured (measured power curve)	Standard uncertainty in AEP	Standard uncertainty in AEP	AEP-extrapolated (extrapolated power curve)	
[m/s]	[kWh]/year	[kWh]/year	%	[kWh]/year	
4	1.148	0.273	23.75%	1.148	COMPLETE
5	2.668	0.414	15.53%	2.668	COMPLETE
6	4.690	0.558	11.90%	4.694	COMPLETE
7	6.966	0.682	9.78%	7.009	COMPLETE
8	9.217	0.776	8.42%	9.414	COMPLETE
9	11.193	0.841	7.51%	11.736	COMPLETE
10	12.735	0.877	6.89%	13.828	INCOMPLETE
11	13.796	0.889	6.45%	15.579	INCOMPLETE

Table 1 shows the power curve at site average air density in a tabular form. This table is complete up to bin 16.5 m/s in accordance with IEC-61400-12-H, which requires 10 minutes of sampled data recorded in 1 minute data sets. Bins above 16.5m/s are incomplete, but were included in the table as reference values. In a final power curve report this situation is not allowable.

Table 2 shows the annual energy production (AEP) for average annual wind speeds varying from 4 m/s to 11 m/s. As IEC-61400-12 indicates, AEP is calculated in two ways, one designated "measured" , were it is assumed that no energy is produced for wind speeds out of the range of measured power curve. The other way to calculate AEP is designated " extrapolated", were zero power is assumed for wind speed below the lowest wind speed measured, and constant power for wind between the highest wind speed measured and the cut-out wind speed.
When the difference between the AEP-measured and AEP-extrapolated, for a given annual speed is higher than 5%, the AEP-measured is labeled as "incomplete".

Figure 12 Power curve, uncertainties and AEP (Annual Energy Production) estimate for an INVAP IVS4500 4.5 kW SWT, partial test results at INTI Cutral Có between 2012 and 2013.

INTI produces detailed reports only for the manufacturer who pays for the testing. A short public report, including the power curve and EAP estimate, is made available for the tested machines. The methodology for developing competence and consistent testing procedures required a Quality System that adhered to ISO/IEC 17025 [30]. This process was requested by INTI authorities and implemented in the case of PWRC/2 using thorough documentation of all circuitries, activities, and equipment or software updates. The INTI Test Site has participated in numerous international initiatives with other laboratories, such as CIEMAT in Spain and INEE in Mexico through the SWTOMP initiative [31] and CYTED-funded REGEDIS network [32], which enabled publications such as [33] in MDPI-Energies Journal in 2022.

3.7 The Evolution Towards Grid-Connected SWT Testing

Small-scale wind energy, despite the growing competition from solar photovoltaic systems, continues to have significant economic importance, especially in areas with good wind resources. Several local manufacturers producing traditional equipment for battery charging and isolated point charging currently offer versions for grid connection [14], mostly without storage. Since the end of 2017, modifications have had to be made to the PWRC/2 measurement equipment for this type of measurement, carrying out a series of cost assessments and adaptation of sensors considering the type of inverter, working voltage, and nominal power of the SWTs.

The first set of sensors contemplated the addition of an isolation amplifier at the high voltage input, initially with ABB 2.5 kW (voltage range 90 to 500 Vdc) and Omnik 1.5 kW (60 to 400 Vdc) grid-connection inverters. This modified the input circuit for measuring these voltages and powers, considering the possibility of having a direct current connection with floating voltages and achieving galvanic isolation (using an AD202 sensor) while maintaining high linearity and precision.

An alternative assembly with better galvanic isolation characteristics was obtained when using integrated DIN Rail type Hall effect sensors (transmitters), capable of converting a direct voltage of

0-600 VDC input to a range of 1 to 5 VDC output, directly compatible with the existing PWRC/2 inputs. Likewise, encapsulated Hall effect current sensors were used to allow different direct current ranges, between 0-5 A, 0-10 A, and 0-20 A. Finally, for direct voltage conversion, 0-600 VDC transmitters were used, model TDVH 660 [34] (YHDC), and for current, Hall effect current sensors in the direct current range 0-20 A, model TDAH. These sensors have a galvanic isolation of 3 kV (50 Hz, 1 min), an accuracy of 1% (TDVH) and 0.5% (TDAH), and a maximum non-linearity of 0.2% in both models. Figure 13 shows the typical connections of these sensors for an SWT being tested coupled to an ABB 2.5 kW inverter in a single-phase, low-voltage connection to the public grid. Figure 14 shows the initial testing of this scheme, comparing the DC output power on the bus bars with the output to the grid using laboratory instruments. The new testing features and continuous maintenance eventually required the installation of high-grade AC-coupled power supplies and RPM sensor channels, as shown in Figure 15.

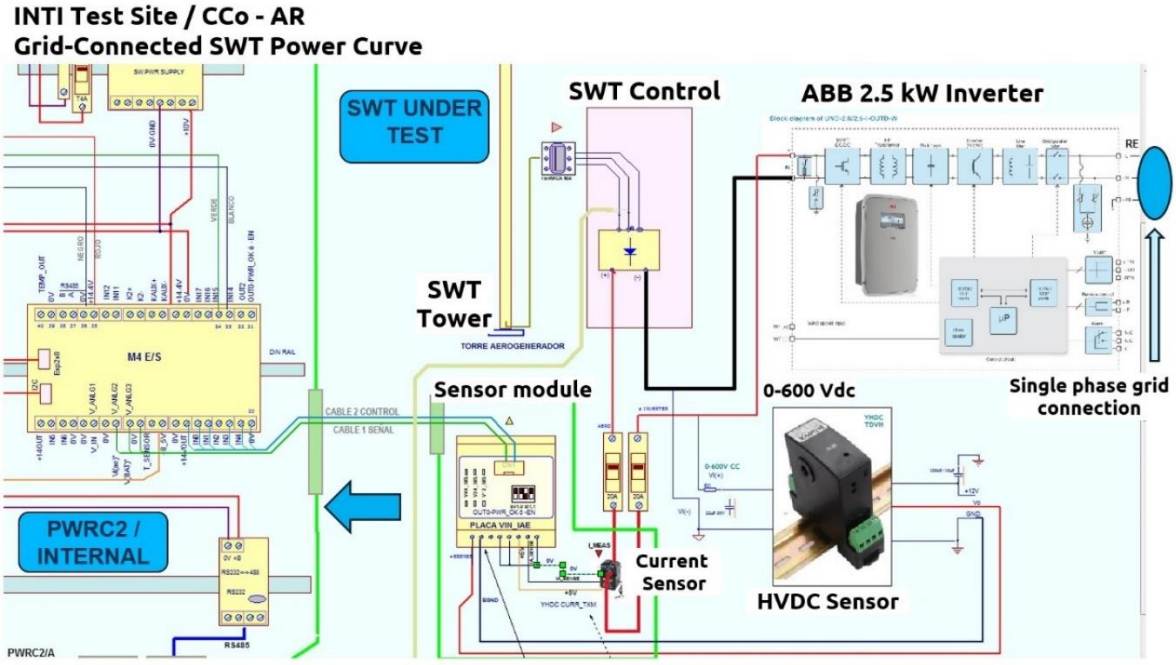

Figure 13 PWRC/2 measurements in grid connection with commercial Hall-effect sensors.

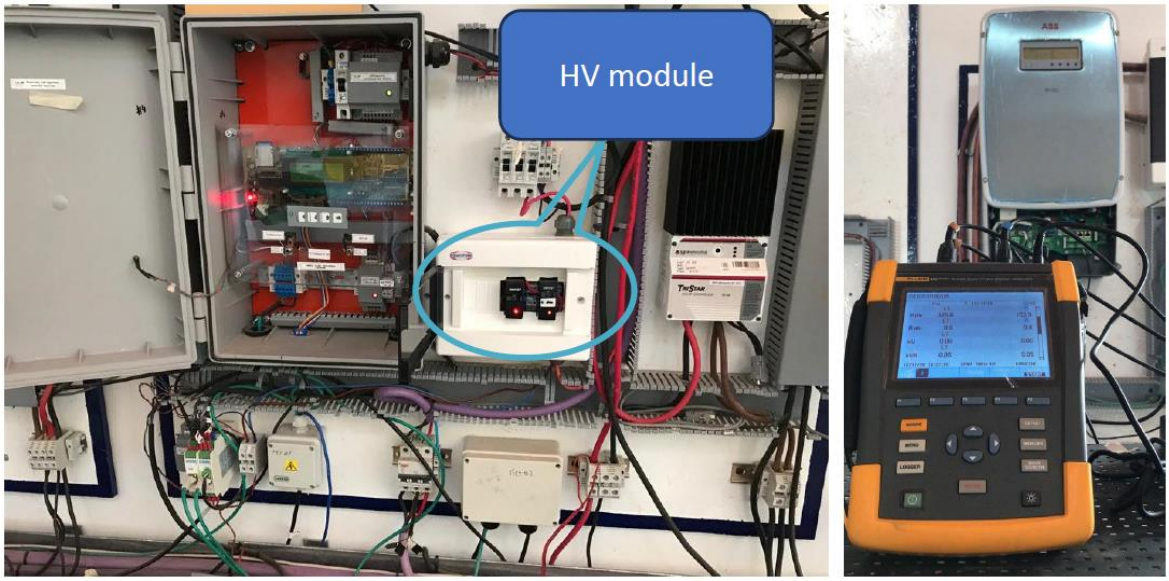

Figure 14 PWRC/2 measurements in grid connection, coupled with an ABB inverter and grid output power instrumentation.

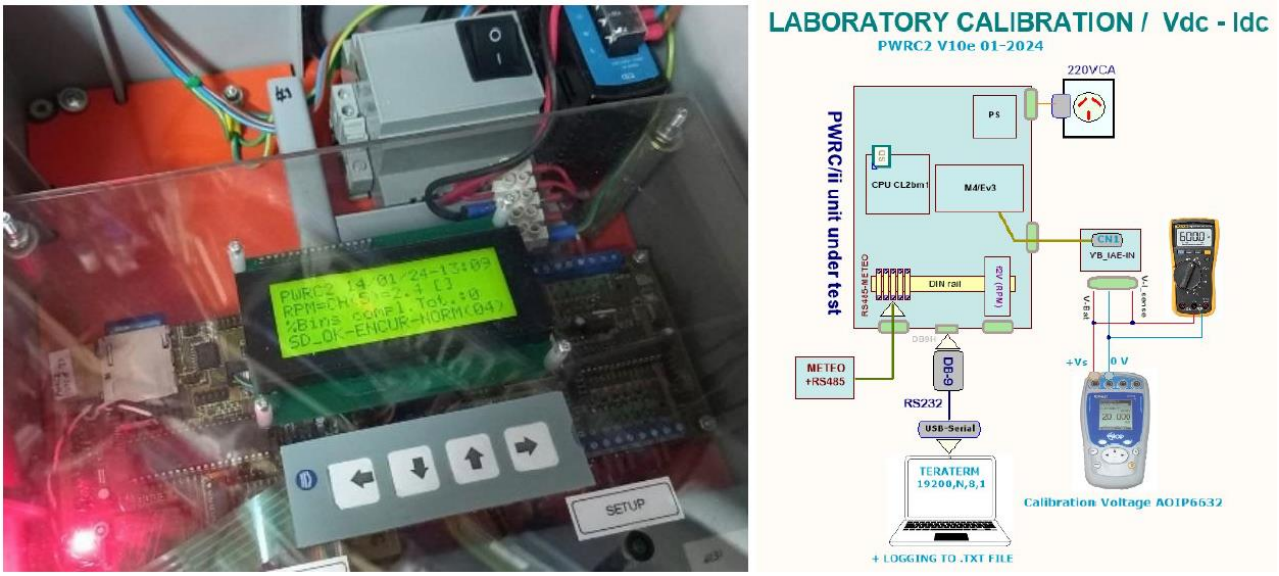

Figure 15 PWRC/2 with recently added AC-coupled power supplies (left), addition of RPM channel with HV input sensor module and (right) regular recalibration of the units.

4. Sound Emissions Testing

These tests aim to characterize the noise emissions of a wind turbine, following the procedures established in the IEC 61400 -11 standard [35]. The methodology seeks to ensure consistency and precision in the measurements, covering acoustic and non-acoustic variables, such as meteorological conditions.

4.1 Acoustic Measurements on SWTs

In this case, measurements are taken with a decibel meter connected to a microphone extension cable placed near the SWT to minimize the influence of external interference, and to obtain the apparent acoustic power level, the levels in third-octave bands, and the tonal quality of the noise.

The microphone, equipped with a windscreen to reduce noise generated by the wind on itself, is positioned at the center and above the perpendicular plane of a 1-meter diameter circular plate, facing the direction opposite to the prevailing wind at the time of measurement, relative to the center of the tower. The microphone axis must point toward the wind turbine (Figure 16, left), and in this measurement position, the plate must be within a wind direction variation range of β = 90°.

The microphone is installed from the axis (vertical) at the center of the wind turbine tower. The microphone position should be at a horizontal distance (Figure 16, right) of:

$$R_0 = H + \frac{D}{2} \quad [m] \tag{10}$$

Where: *H* is the height of the rotor axis, and *D* is the rotor diameter.

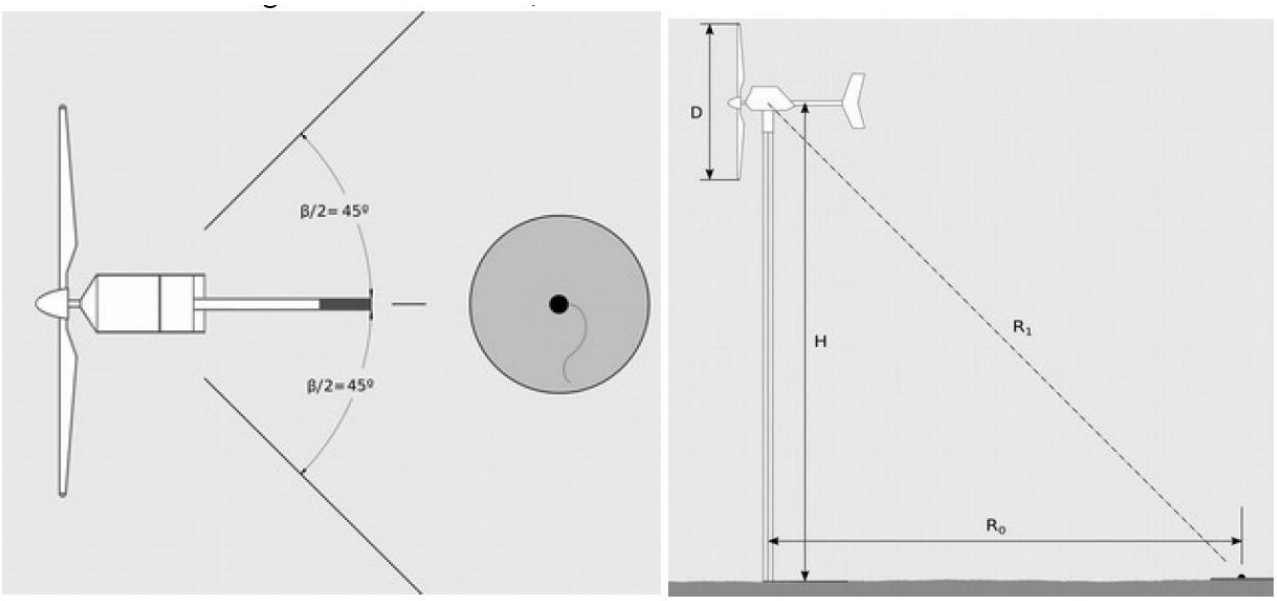

Figure 16 Microphone positioned (left) in the middle of the circular plate. The distance R_0 is calculated based on Eq.10.

To measure the sound power level, an A-weighting is used [35, 36]. The equivalent continuous level is calculated by averaging the sound energy (in dB(A)) over 10-second periods, which allows the noise variability according to the wind speed to be captured. The frequency spectrum is also measured in third-octave bands, from 20 Hz to 10 kHz.

It is crucial to perform a background noise measurement (Figure 17) when the wind turbine is not in operation, to be able to discriminate the noise generated only by the wind turbine from the other noise sources present.

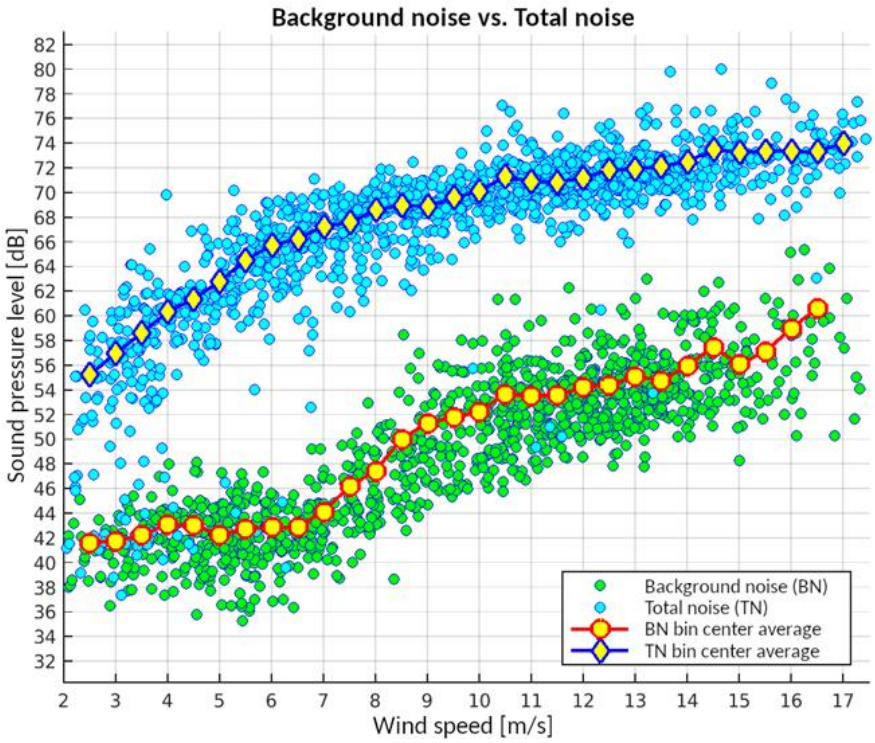

Figure 17 Background noise levels (BN) vs total noise (TN).

The noise spectrum corrected by background wind noise measurement (Figure 18) is also measured and presented in graphical form.

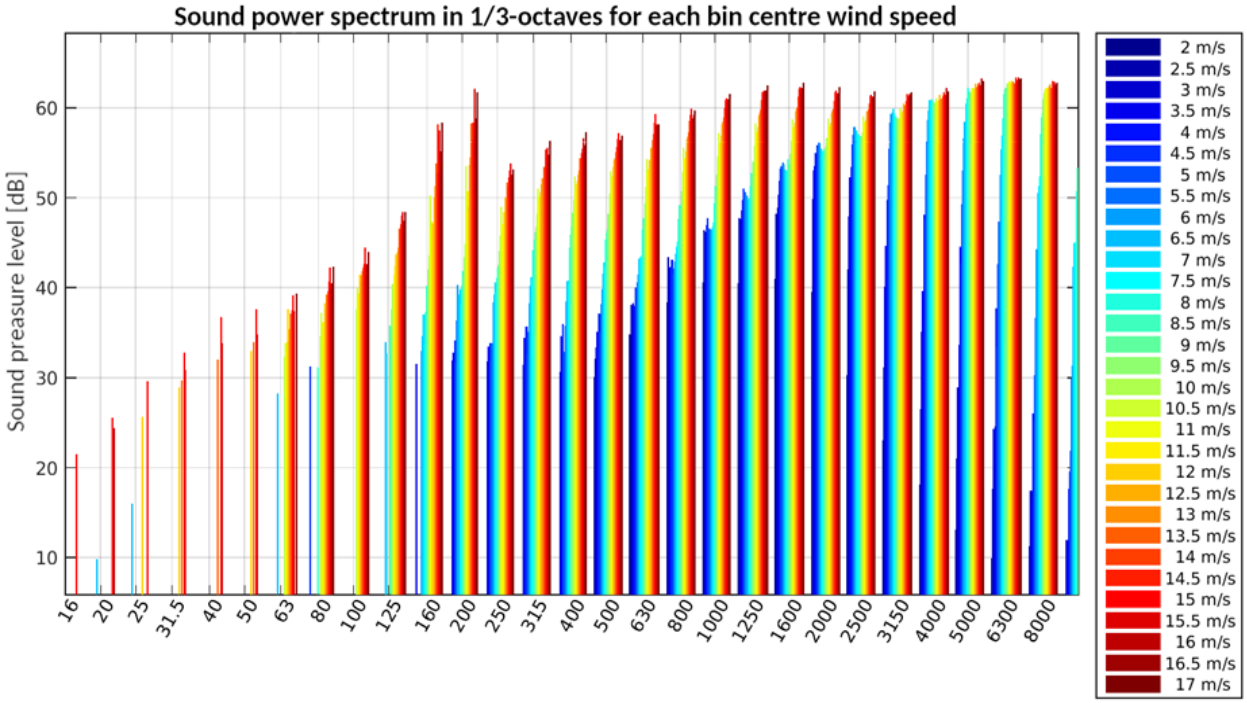

Figure 18 Noise spectrum corrected by background wind noise.

4.2 Non Acoustic Measurements

Wind speed and direction data are recorded, and synchronized with acoustic measurements using a special function in PWRC/2 firmware. The wind direction is assessed within ±45° of the measurement position, maintaining the relevant exclusion sectors.

4.3 Measurement Processing

Acoustic and non-acoustic measurements are processed according to the guidelines of the standard. Wind speed is adjusted considering the roughness of the terrain and the height of the anemometer. Noise measurements are corrected for background noise, subtracting the latter from the total noise to obtain the noise emitted only by the wind turbine.

4.4 Results in Sound Measurements

The data obtained are presented in tables and graphs, including the noise spectrum and the apparent sound power as a function of wind speed (Figure 19, left). An inmission map (Figure 19, right) is also included, showing the variation of the sound pressure level with distance from the wind turbine at different wind speeds. The final report must show the characteristics of the wind turbine, the measurement site, the equipment used, and the data obtained with their corresponding uncertainties.

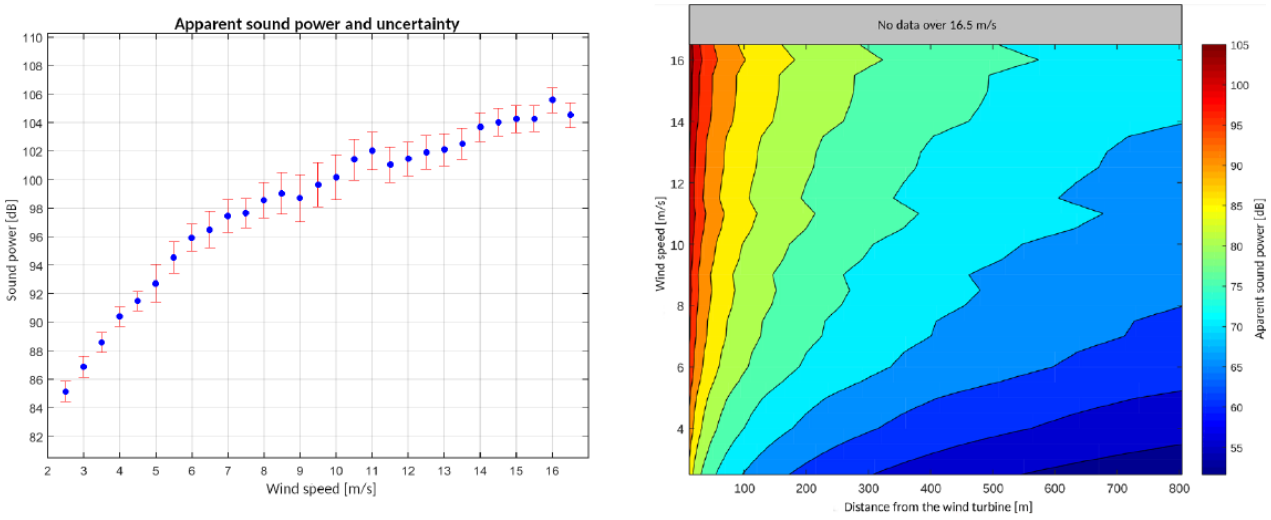

Figure 19 Apparent noise level (including uncertainties) and inmission map, showing the apparent noise level at different distances from the SWT, and for different levels of wind speed.

5. Technical Assistance Cases for SWTs

The INTI Test Site in Cutral Co has performed over a dozen power curve certification tests, some of which were lengthy processes, and a slightly smaller number of technical consultancy contracts with local manufacturers related to limitations or problems with the machines produced. Many of these contracts resulted from the first tests of a specific model at the Test Laboratory. Some of the cases are presented in this section.

5.1 Orientation System Improvement Case

One of the cases presented by local manufacturers was that of a wind turbine that did not reach the design power due to a pronounced orientation error with respect to the direction of the wind. The project's objective was to analyze and correct the orientation to maximize the performance of the SWT.

To measure the orientation error, a special device was constructed. Although a low-cost encoder was evaluated, its implementation was complex, so an absolute encoder based on infrared sensors and a Gray code disk was developed. This device was adapted to the geometry of the nacelle, allowing orientation errors to be monitored as a function of wind speed (Figure 20).

Figure 20 Gray code disk and acquisition system, mounting on the SWT (a 2.6 m diam., PM generator rated at 0.8 kW).

Subsequently, modifications were made to the area and anchoring system of the orientation vane. These changes corrected the orientation of the wind turbine, evidenced by an increase in power that reached levels close to the nominal design power.

Improvements in the orientation system made it possible to correct the disorientation and raise the power output of the wind turbine to design levels (Figure 21). The implementation of the absolute encoder and the modifications to the vane achieved an optimized machine performance.

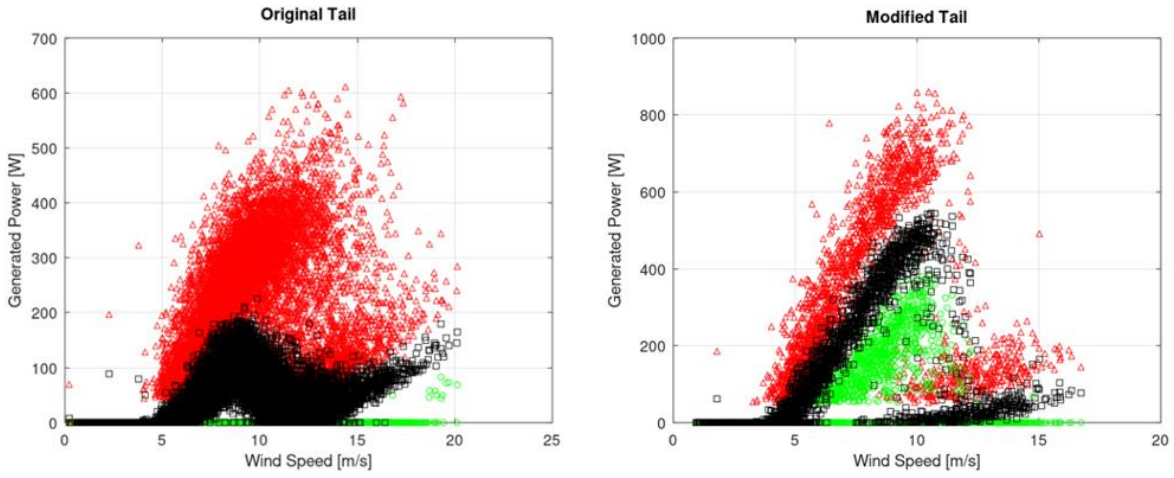

Figure 21 Power performance of the 2.6 m diam. SWT with original orientation vane (left), and significant power gains (right) with design corrections performed at INTI Test site.

5.2 Reduction of Noise Emissions

Another case presented by a local manufacturer was an SWT that produced sound emissions in different frequency ranges depending on the wind speed: at low frequencies for high wind speeds and at higher frequencies at intermediate speeds. To reduce these emissions, a study focused on the mechanisms of self-produced noise generation in aerodynamic profiles was performed.

The causes of the emissions were identified, and for each noise generation mechanism, modifications to the profile surface were implemented. These modifications were evaluated by measuring sound emissions before and after the intervention. The results showed an improvement in noise reduction, without affecting power generation performance.

Improvements in noise reduction proposed changes in the blade construction process. However, these changes were not addressed within the framework of this technical assistance. The following cases address the results of the noise emissions measurements before and after the modifications made.

1. Laminar Boundary Layer Noise: Attenuation is achieved by transforming the laminar boundary layer into a turbulent layer (Figure 22).

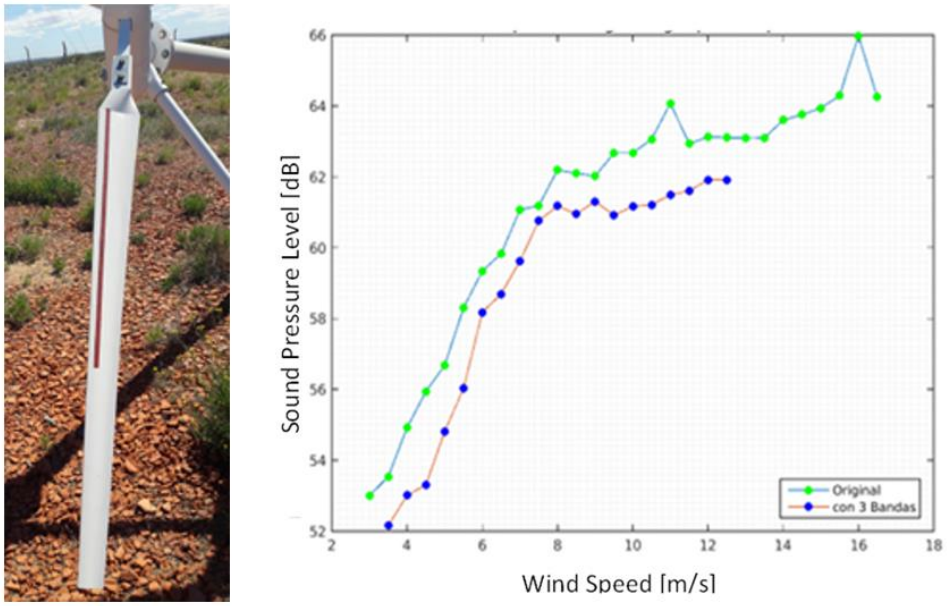

Figure 22 Noise reduction on the SWT, by profile modification.

2. Trailing Edge Thickness Noise: To reduce this noise, the thickness of the trailing edge must be less than the thickness of the boundary layer at that point (Figure 23).

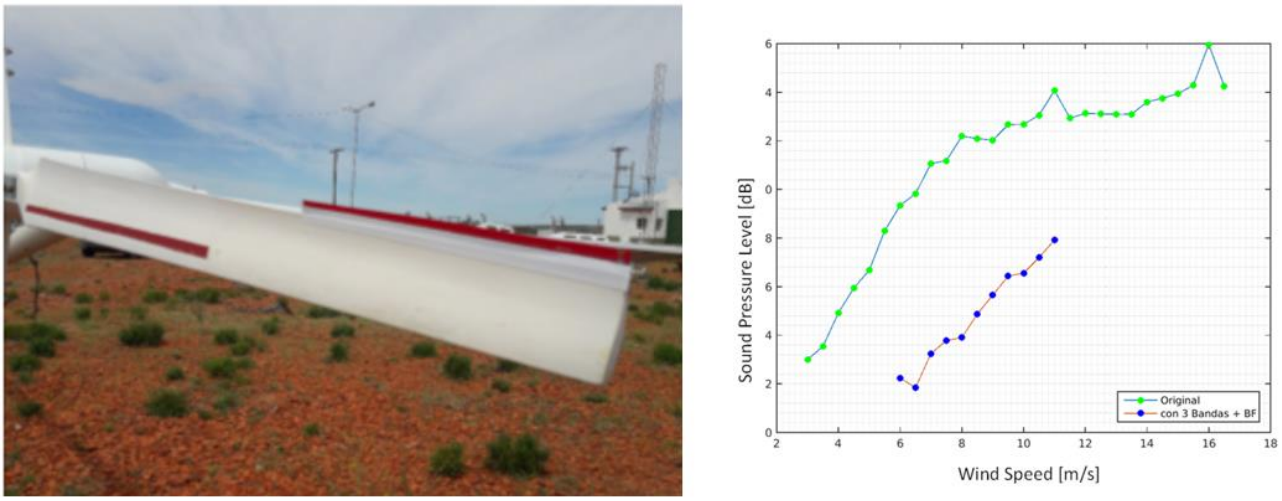

Figure 23 Noise reduction on the SWT, by the modified thickness of the trailing edge.

5.3 Use of Solar Inverter for Grid Injection with Wind Turbine

This technical assistance was performed in agreement with UTN-FRN (Universidad Tecnológica Nacional, Facultad Regional Neuquén) and with the cooperation of the Energy Studies Group (GESE) headed by Mg. Ing. Ruben Bufanio and Mg. Ing. Damián Marasco, based on their power electronics expertise and work on SWT emulation [37]. The results of this assistance were published in Energies [33]. The objective of this case was to explore the use of a low-cost solar inverter for injection into the electrical grid, associated with a wind turbine. This type of combination seeks to maximize the efficiency and viability of renewable energy.

To address this problem, it has been observed [33] that the algorithm in many solar inverter control systems tends to demand more significant current if voltage is maintained constant on the DC bus. When coupled to a SWT, this causes:

- Increased resistant electrical torque.
- Decrease in rotor rotation speed.
- Drop in system performance.

This can be appreciated in Figure 24 where an initial comparison between the performance of identical PM SWTs in battery charging configuration compared to grid injection through an inverter. The square dots of the grid-injection case show most of the measurements in the extremely low-power region.

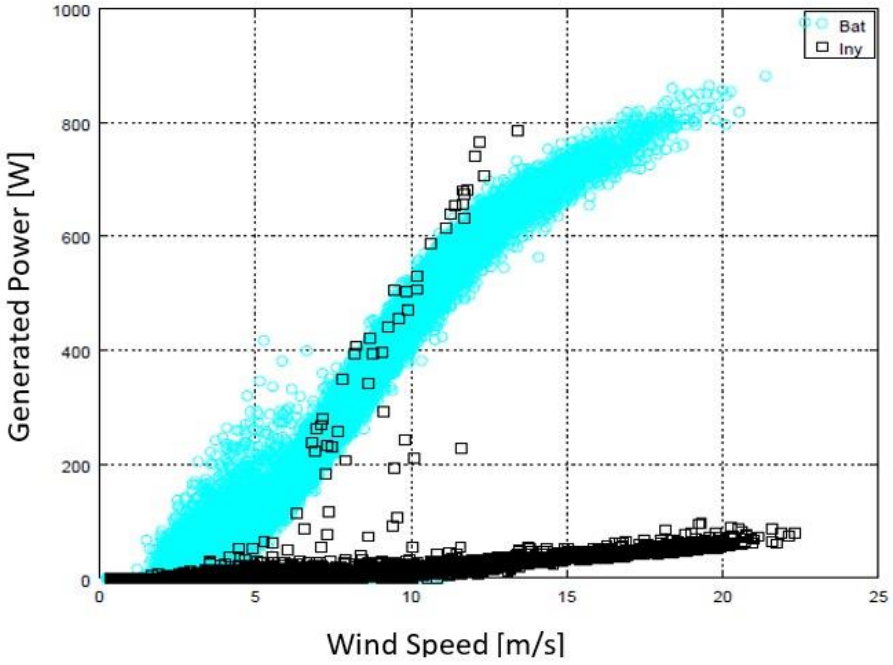

Figure 24 Initial comparison of battery bank generation (Bat) vs. grid injection (Iny).

Wind-inverters have a power-voltage control curve that optimizes the rotor speed depending on the wind speed, but tend to be costly. To integrate a low-cost and readily available solar inverter into the system, an overvoltage crowbar power board was designed by the GESE group together with a mobile (Android) application, both shown in Figure 25.

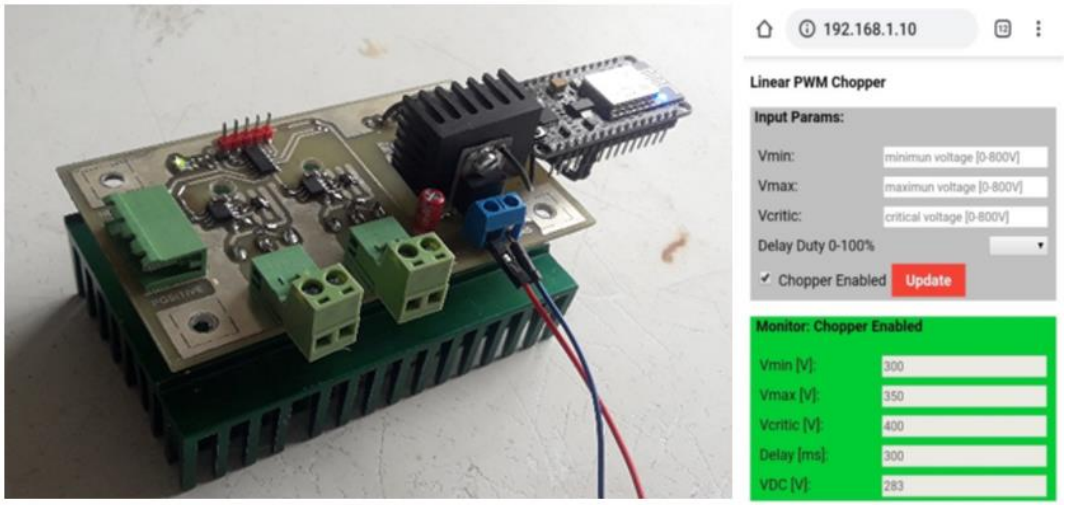

Figure 25 Power board for overvoltage control and associated app developed by GESE/UTN FRN.

This device, connected to the DC bus before the input to the inverter, allows for:

- Disconnection of the load on the rotor.
- Adaption of power generation.

A comparison of the performance of the system was carried out using two modalities:

1. Grid Injection: Using the solar inverter linked to the wind turbine, adjusting voltage limits.

2. Battery Bank: Isolated operation using a battery system.

The results demonstrated that the SWT with grid injection system implementing the GESE bypass board exceeded the performance of the battery bank system, thus achieving an improvement in energy generation. This can be appreciated for two limit voltages of 100 and 200 V, compared to the battery-charging case in Figure 26.

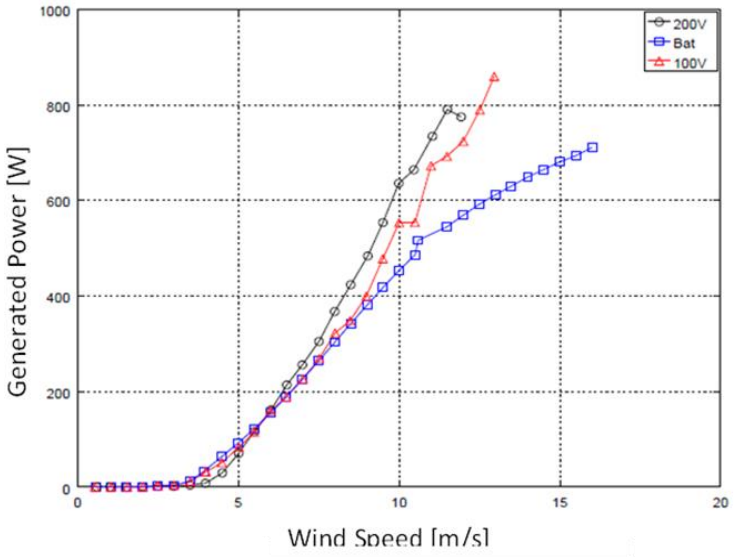

Figure 26 Comparison of power curves with grid inverter + GESE board, vs. battery-isolated system.

5.4 Cooperation with Manufacturers Regarding the Use of Technology

As a simultaneous program with the development of the measurement and testing laboratory, cooperation with a group of national manufacturers allowed for the release in 2016 of two publicly open documents, related to SWTs (Figure 27). The first is a general guide for SWT potential or current users, aimed at providing information on the use of wind energy as a power alternative. This document addresses aspects related to the wind resource, loads and consumption characteristics, and application cases provided by the manufacturers.

Figure 27 Information and installation manuals published in 2016 by INTI and SWT manufacturer associations, and INTI SWT installer certification scheme [38].

The second document is aimed at installing SWT equipment, divided into two sections. The first section is focused on the mechanical aspects of the installation. Among them, are tower assembly, fastening elements, leveling techniques, assembly of anchors, etc. The second section is dedicated to details of electrical installations in small wind systems.

Additionally, a certification scheme for SWT installers was implemented in accordance with the ISO 17024 [39] standard for certification of people and cooperation with the INTI certification body. The objective of this activity is to have qualified technical personnel to ensure the successful installation of SWTs since many of the failures in renewable systems are a consequence of mistakes in the installation process. Documents and certification schemes are available in [38].

6. Conclusions

The process of surveying the industry of manufacturing low-power wind turbines in Argentina led to the implementation by INTI of a laboratory to carry out tests following IEC 61400-12-1 standards. During the test implementation process, operating measurements of the equipment were obtained that warranted making various improvements to the products. In some cases, these tests derived in technical assistance contracts that enabled manufacturers to match the announced performance of the products offered. For many of these improvements, the development of technical capabilities was required in addition to implementing test methods under the IEC 61400 standards and a laboratory Quality System under IEC 17025.

The possibility of adopting previous academic developments and measurement systems made it possible to capitalize on the experience in low-power wind energy gained from previous projects. The installation of the laboratory, implementation of tests under IEC61400-12-1 standards, and the possibility of cooperating with the SWT manufacturers have made it possible to achieve technical improvements to the designs aimed at increasing reliability and reducing the cost of the products. More than a dozen SWT tests (half of them with public reports), slightly fewer technical assistance contracts, and numerous certifications, documentation, and SWT awareness activities are important achievements of the INTI Cutral Co SWT Test Laboratory.

Future activities within the laboratory will be based on the expansion of technical capabilities and the addition of equipment suitable for use in grid-connected SWTs and hybrid systems.

Acknowledgments

Authors are thankful to their respective institutions for supporting research in the areas of the present work. A special recognition for the Cutral-Co Municipality, for UTN-FRN and their GESE group and for former INTI Energy group leaders Guillermo Martin and Juan Pablo Duzdevich who had a decisive role in pioneering the work to install the SWT-Testing Lab.

Author Contributions

Conceptualization; methodology: R.O., A.Z., M.A.; visualization, review, and editing: G.C.; formal analysis; investigation; resources and data curation; writing—original draft preparation: R.O., A.Z., M.A. supervision; project administration: A.Z., M.A. All authors have read and agreed to the published version of the manuscript.

Funding

INTI (National Institute of Industrial Technology), UNPA (Universidad Nacional de la Patagonia Austral).

Competing Interests

The authors have declared that no competing interests exist.

References

1. International Electrotechnical Commission. Wind Turbines–Part 12-1: Power Performance Measurements of electricity producing wind turbines [Internet]. Geneva, Switzerland: International Electrotechnical Commission; 2005. Available from: https://webstore.iec.ch/en/publication/5429.
2. International Electrotechnical Commission. Wind Turbines, Part 2: Small Wind Turbines [Internet]. Geneva, Switzerland: International Electrotechnical Commission; 2013. Available from: https://webstore.iec.ch/en/publication/5433.
3. Oliva R, Salvador J, González JF, Cortez N, Lescano J, Triñanes P, et al. La normativa IEC para sistemas eólicos e híbridos aislados, y la utilización de tecnologías de medición remota: Aplicación en contexto patagónico [Internet]. Salta, Argentina: Asociación Argentina de Energías Renovables y Medio Ambiente; 2021. Available from: https://portalderevistas.unsa.edu.ar/index.php/averma/article/download/2418/2330.
4. Bowen A, Huskey A, Link H, Sinclair K, Forsyth T, Jager D. Small Wind Turbine Testing Results from the National Renewable Energy Laboratory [Internet]. Golden, CO: National Renewable Energy Laboratory; 2010. Available from: https://www.nrel.gov/docs/fy10osti/48089.pdf.
5. Migliore P, van Dam J, Huskey A. Acoustic tests of small wind turbines [Internet]. Golden, CO: National Renewable Energy Laboratory; 2004. Available from: https://www.nrel.gov/docs/fy04osti/34662.pdf.
6. ICC-Small Wind Certification Council. Standards [Internet]. Country Club Hills, IL: ICC-Small Wind Certification Council; 2024. Available from: https://smallwindcertification.org/resources/standards/.
7. Whale J, Pryor T. The ResLab Small Wind Program [Internet]. Murdoch, WA: Murdoch University; 2005. Available from: https://researchportal.murdoch.edu.au/esploro/outputs/conferencePaper/The-ResLab-small-wind-program/991005542319507891.
8. Whale J, McHenry MP, Malla A. Scheduling and conducting power performance testing of a small wind turbine. Renew Energy. 2013; 55: 55-61.
9. Arribas L. Testing and certification for small wind turbines (SWT): Challenges and actions to address them [Internet]. Madrid, Spain: CIEMAT; 2012. Available from: https://www.irena.org/-/media/Files/IRENA/Agency/Events/2012/Oct/24/5_Luis_Maria_Arribas.pdf?la=en&hash=A51E2EA6B5B63EACB27E3DAFC16FC28BC5DB3716.
10. Intertek. Intertek signs partnership agreement with CIEMAT the Spanish Ministry of Economy and Competitiveness research centre [Internet]. Bilbao, Spain: Intertek; 2013. Available from: https://www.intertek.com/news/2013/01-14-partnership-with-ciemat/.
11. Intertek. Intertek gains accreditation for small scale wind testing [Internet]. Kista, Sweden: Intertek; 2013. Available from: https://www.intertek.com/news/2013/05-30-small-scale-wind-testing-accreditation/.

12. Martin G, Duzdevich J, Oliva R. Instalación y avances en Plataforma de Ensayo para Pequeños Aerogeneradores [Internet]. Salta, Argentina: Asociación Argentina de Energías Renovables y Medio Ambiente; 2012. Available from: https://portalderevistas.unsa.edu.ar/index.php/averma/article/download/2180/2107/5096.
13. IEA Wind. IEA Wind RP for Consumer Labelling of Small Wind Turbines [Internet]. Roskilde, Denmark: IEA Wind; 2011. Available from: https://iea-wind.org/task27/.
14. Argentina.gob.ar. Law 27424 (2018) to Promote the Generation of Energy from Renewable Sources for Self-Consumption and the Injection of Surpluses into the Grid in Argentina [Internet]. Argentina.gob.ar; 2018. Available from: https://www.argentina.gob.ar/economia/energia/generacion-distribuida.
15. Oliva R. Introducción a los modelos y control de máquinas eólicas [Internet]. Ediciones Universidad Nacional de la Patagonia Austral; 2011. Available from: https://en.energiasalternativas-unpa.net/publicaciones.
16. Manwell JF, McGowan JG, Rogers AL. Wind energy explained: Theory, design and application. 2nd ed. John Wiley & Sons; 2009.
17. Oliva RB, Vallejos R. Requerimientos para la evaluación de curvas de potencia en aerogeneradores de baja potencia para carga de baterías. Proceedings of the XXIX Congreso de ASADES; 2006 October 23-27; Buenos Aires, Argentina. Salta, Argentina: Asociación Argentina de Energías Renovables y Medio Ambiente.
18. MEASNET. Measuring Network of Wind Energy Institutes: Power Performance Measurement Procedure—Version 5 [Internet]. Madrid, Spain: MEASNET; 2009. Available from: http://www.measnet.com/documents/.
19. MEASNET. Measuring Network of Wind Energy Institutes: Anemometer Calibration Procedure—Version 2 [Internet]. Madrid, Spain: MEASNET; 2009. Available from: http://www.measnet.com/documents/.
20. Modbus Protocol. Application-layer open messaging protocol [Internet]. Skive, Denmark: Modbus Protocol; 2025. Available from: https://modbus.org/specs.php.
21. Mattio HF, Tilca F. Recomendaciones para mediciones de velocidad y dirección de viento con fines de generación eléctrica, y medición de potencia eléctrica generada por aerogeneradores [Internet]. INENCO; 2009. Available from: https://www.inenco.unsa.edu.ar/energia-eolica/.
22. Oliva R, Cortez N, Jones RD. Procesamiento de mediciones de potencia eléctrica en pequeños sistemas eólicos domiciliarios [Internet]. Salta, Argentina: Asociación Argentina de Energías Renovables y Medio Ambiente; 2008. Available from: https://sedici.unlp.edu.ar/handle/10915/94627.
23. L&R INGENIERÍA. CL2bm1 CPU Boards and integration to PWRC/2 units [Internet]. Río Gallegos, Argentina: L&R INGENIERÍA: Available from: https://www.lyringenieria.com.ar/language/en/downloads/.
24. Oliva RB. Hardware and firmware design and implementation of twin 8-bit and 32-bit microcontroller boards for research and educational applications. IEEE Embed Syst Lett. 2022; 15: 65-68.
25. ISO. ISO/IEC Guide 98-1, Uncertainty of measurement - Part 1: Introduction to the expression of uncertainty in measurement [Internet]. Geneva, Switzerland: ISO; 2009. Available from: https://www.iso.org/standard/46383.html.

26. Gupta SV. Measurement uncertainties: Physical parameters and calibration of instruments. Berlin: Springer Science & Business Media; 2012.
27. Oliva R. Estación Meteorológica de construcción modular orientada a la prospección eólica en Argentina. Salta, Argentina: Universidad Nacional de Salta; 2012.
28. Zappa A, Oliva R, Duzdevich J, Martín G. Evaluación de curva de potencia en plataforma de ensayo para aerogeneradores de baja potencia. Proceedings of the XXXVI Reunión de Trabajo de la Asociación Argentina de Energías Renovables y Ambiente; 2013 October 22-25; Tucumán, Argentina. Salta, Argentina: Asociación Argentina de Energías Renovables y Medio Ambiente.
29. Oliva R. Evaluación de incertidumbre en mediciones de potencia eléctrica en registradores automáticos - Caso de implementación para medición de curva de potencia de pequeños aerogeneradores. Proceedings of the CASE 2014; 2014 August 13-15; Facultad de Ingeniería (UBA), Argentina.
30. ISO. ISO/IEC 17025–General requirements for the competence of testing and calibration laboratories [Internet]. Geneva, Switzerland: ISO; 2017. Available from: https://www.iso.org/publication/PUB100424.html.
31. CIEMAT. Small Wind Turbines Optimization and Market Promotion Project Web Page [Internet]. Madrid, Spain: CIEMAT. Available from: http://swtomp.ciemat.es/.
32. CYTED. REGEDIS–Red de energía eólica para la generación distribuida en el ámbito urbano (718RT0565) [Internet]. Madrid, Spain: CYTED; 2025. Available from: https://cyted.org/REGEDIS.
33. Bufanio R, Arribas L, de la Cruz J, Karlsson T, Amadío M, Zappa AE, et al. An update on the electronic connection issues of low power SWTs in AC-coupled systems: A review and case study. Energies. 2022; 15: 2082.
34. YHDC. DC Voltage Transducer – Hall Effect 0-660 V 3 kV isolation [Internet]. Piastów, Poland: YHDC. Available from: https://www.poweruc.pl/collections/transmitter.
35. International Electrotechnical Commission. Wind turbines - Part 11: Acoustic noise measurement techniques [Internet]. Geneva, Switzerland: International Electrotechnical Commission; 2012. Available from: https://webstore.ansi.org/standards/iec/iec6140011eden2012.
36. International Electrotechnical Commission. Wind energy generation systems - Part 11-2: Acoustic noise measurement techniques - Measurement of wind turbine sound characteristics in receptor position [Internet]. Geneva, Switzerland: International Electrotechnical Commission; 2024. Available from: https://webstore.iec.ch/en/publication/62414.
37. Zuñiga C, Bufanio R, Marasco D, Monte G, Scarone N, Agnello A. Estudio y desarrollo de banco de emulación de turbina eólica de baja potencia. Proceedings of the IV Congreso Energías Sustentables Bahia Blanca; 2023 March 15-18; Buenos Aires, Argentina.
38. INTI. SWT Certification and documentation [Internet]. Buenos Aires, Argentina: INTI. Available from: https://www.inti.gob.ar/areas/servicios-regulados/certificaciones/organismo-de-certificacion/tramites/instaladores-de-aerogeneradores-nivel-i.
39. ISO. ISO/IEC 17024 Conformity assessment—General requirements for bodies operating certification of persons [Internet]. Geneva, Switzerland: ISO; 2012. Available from: https://www.iso.org/standard/52993.html.